Supplementary Material

Structure and spectroscopic properties of etherates of the beryllium halides

Deniz F. Bekiş, Lewis R. Thomas-Hargreaves, Chantsalmaa Berthold, Sergei I. Ivlev and Magnus R. Buchner*

Table of Contents

1 NMR Spectroscopic Data S1

2 Vibrational Spectroscopic Data S37

1 NMR Spectroscopic Data

1.1 $[BeCl_2(OEt_2)_2]$ (1a):

1.1.1 Solvent – Et_2O

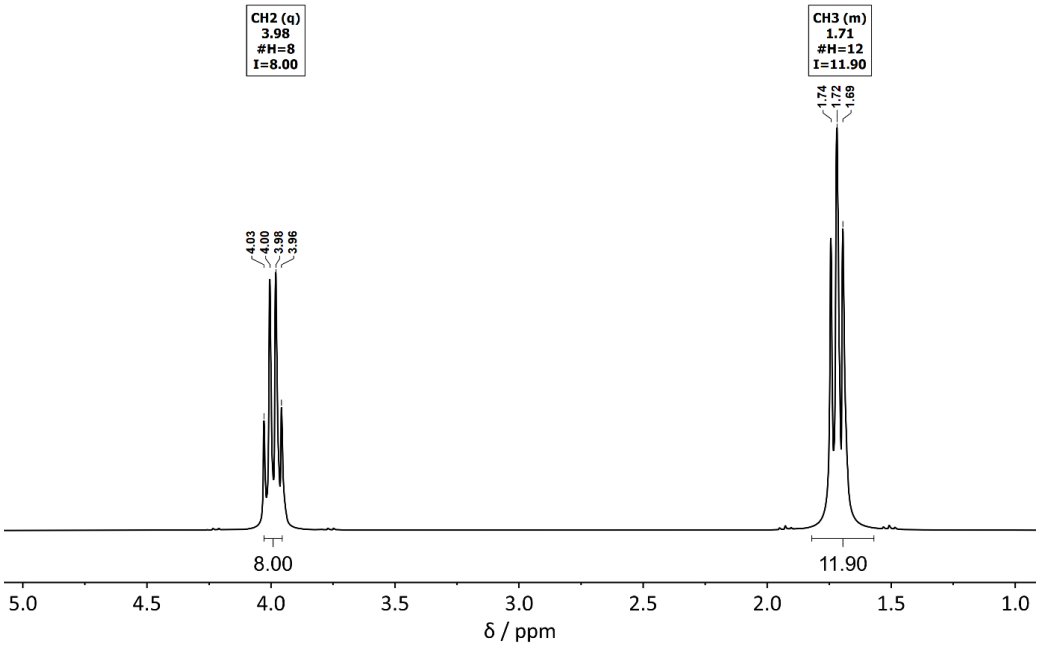

Figure 1: ^{1}H NMR spectrum of $[BeCl_2(OEt_2)_2]$ (**1a**) in Et_2O at T = 300 K.

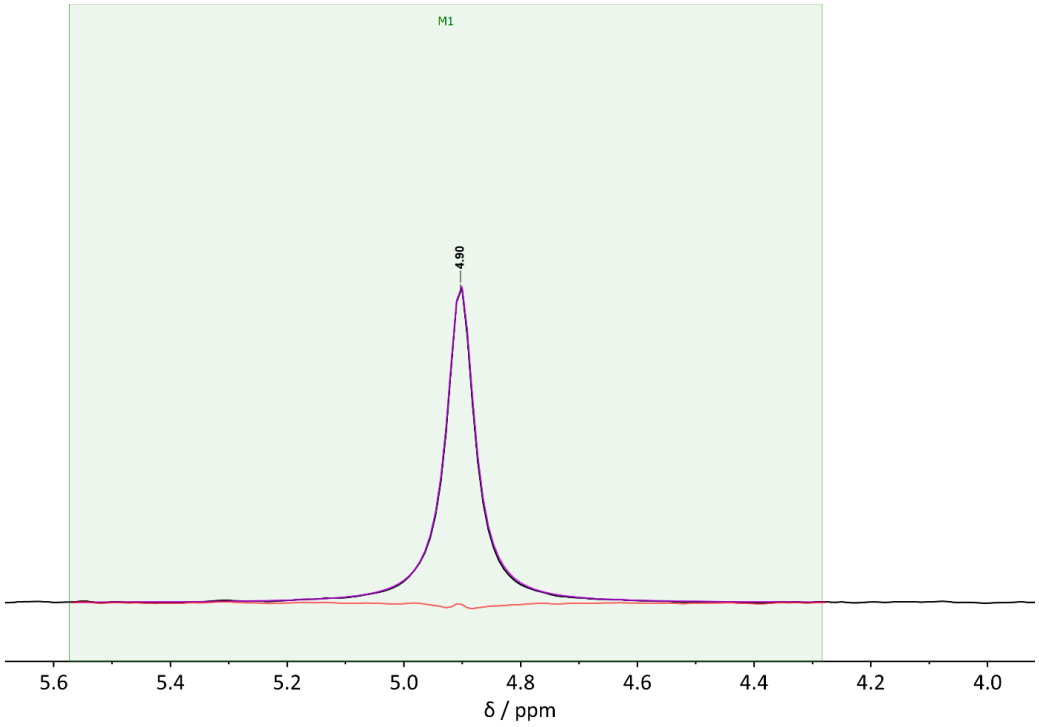

Figure 2: ^{9}Be NMR spectrum of $[BeCl_2(OEt_2)_2]$ (**1a**) in Et_2O at T = 300 K. Line fitting profiles (purple) and differential plot of calculated *versus* observed line (red) profiles are marked.

1.1.2 Solvent – C_6D_6

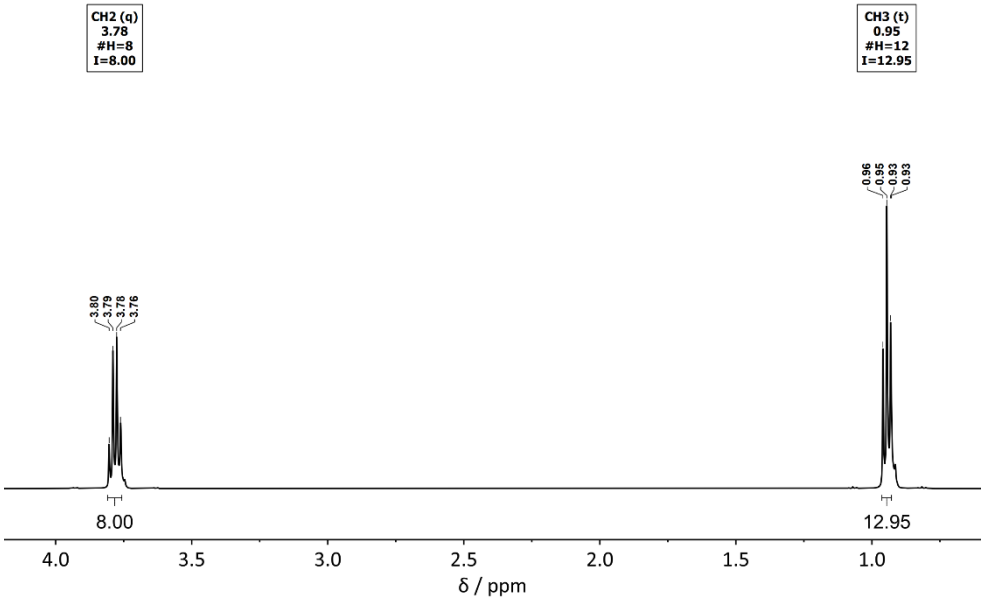

Figure 3: ^{1}H NMR spectrum of $[BeCl_2(OEt_2)_2]$ (**1a**) in C_6D_6 at T = 300 K.

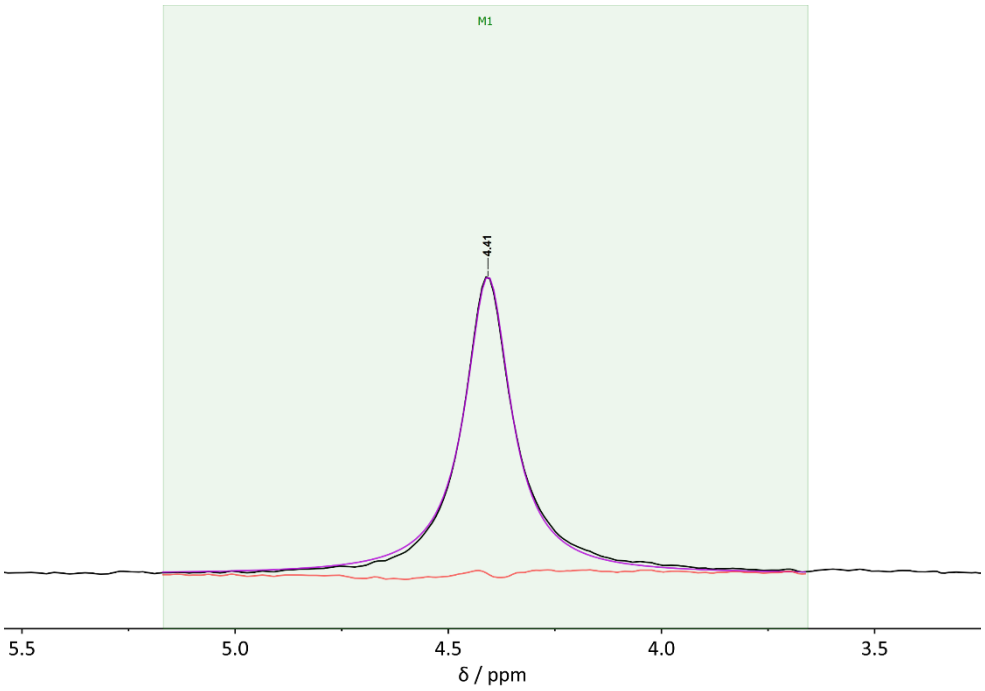

Figure 4: ^{9}Be NMR spectrum of $[BeCl_2(OEt_2)_2]$ (**1a**) in C_6D_6 at T = 300 K. Line fitting profiles (purple) and differential plot of calculated *versus* observed line (red) profiles are marked.

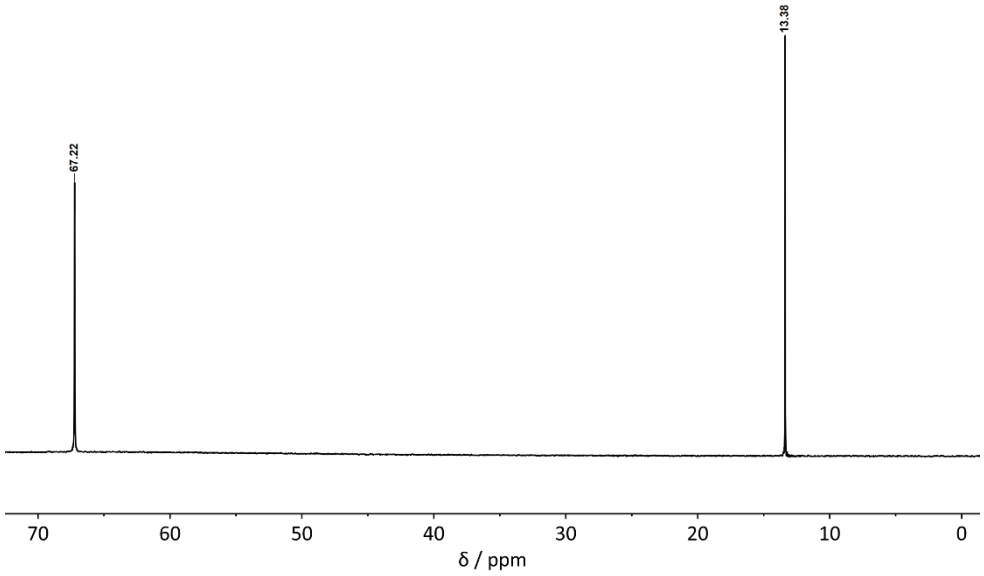

Figure 5: $^{13}C\{^{1}H\}$ NMR spectrum of $[BeCl_2(OEt_2)_2]$ (**1a**) in C_6D_6 at T = 300 K.

1.1.3 Solvent – CD_2Cl_2

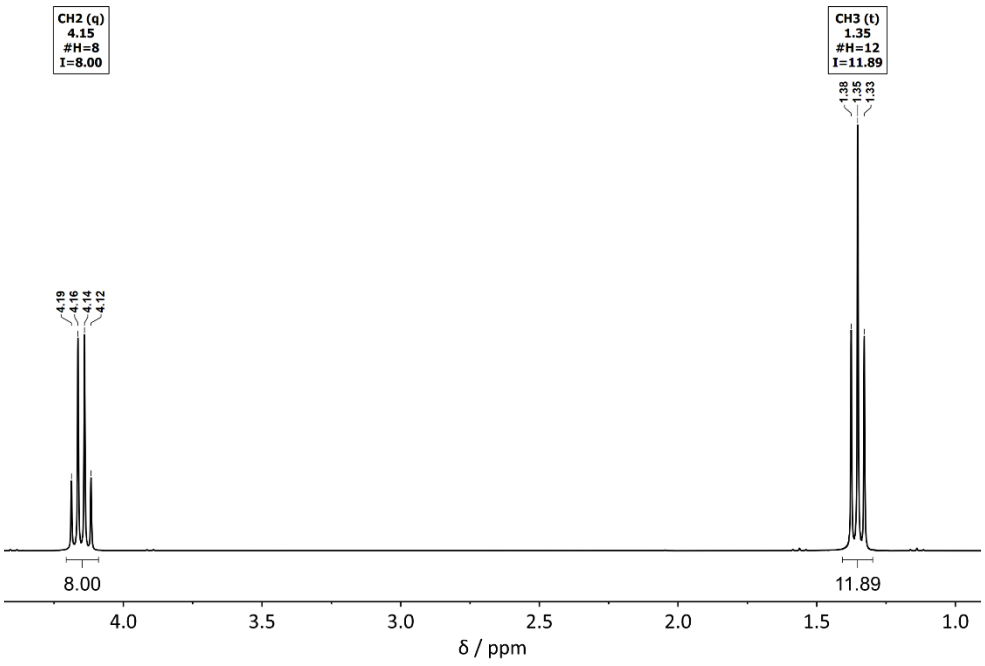

Figure 6: ^{1}H NMR spectrum of $[BeCl_2(OEt_2)_2]$ (**1a**) in CD_2Cl_2 at T = 300 K.

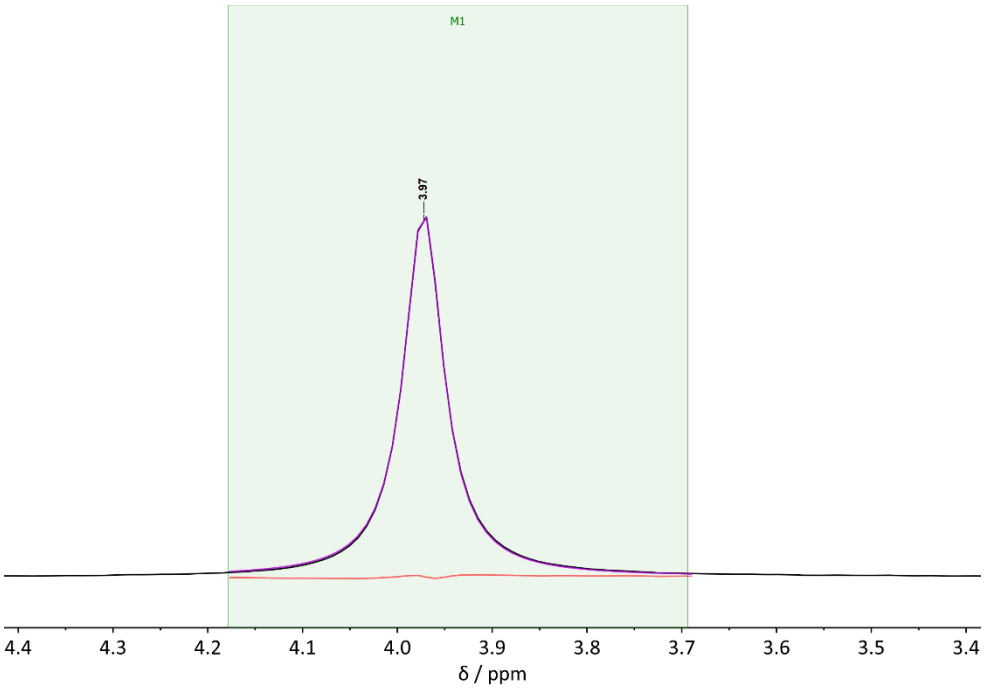

Figure 7: ^{9}Be NMR spectrum of [$BeCl_2(OEt_2)_2$] (**1a**) in CD_2Cl_2 at *T* = 300 K. Line fitting profiles (purple) and differential plot of calculated *versus* observed line (red) profiles are marked.

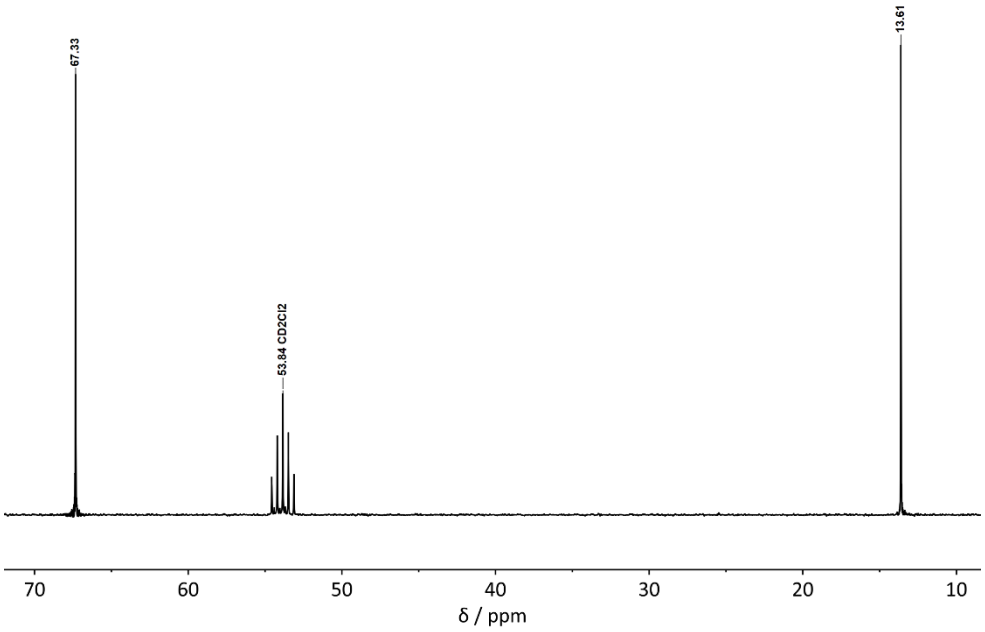

Figure 8: $^{13}C\{^{1}H\}$ NMR spectrum of [$BeCl_2(OEt_2)_2$] (**1a**) in CD_2Cl_2 at *T* = 300 K.

1.1.4 Solvent – $CDCl_3$

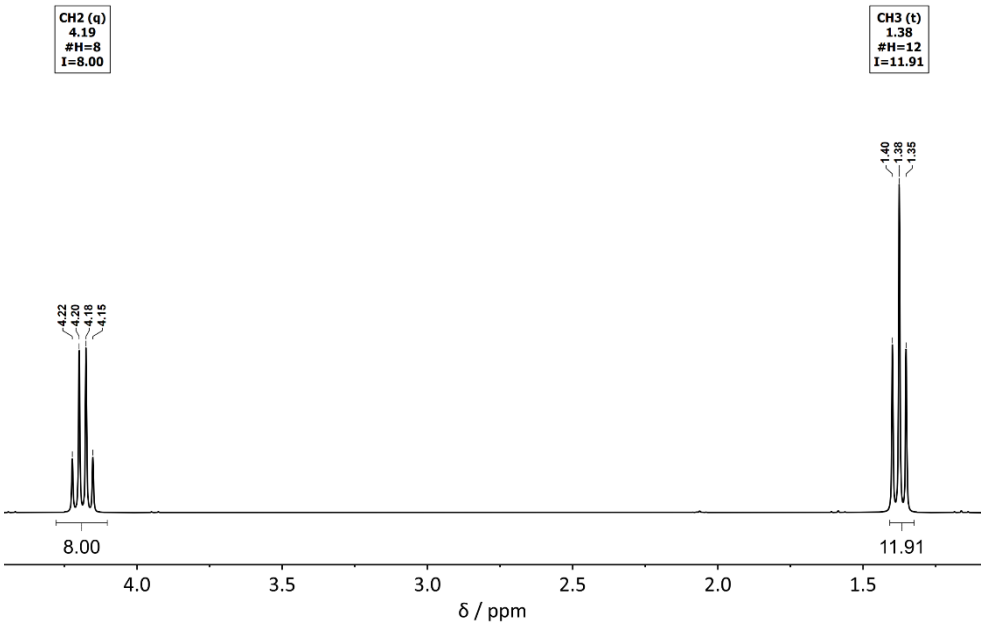

Figure 9: ^{1}H NMR spectrum of $[BeCl_2(OEt_2)_2]$ (**1a**) in $CDCl_3$ at T = 300 K.

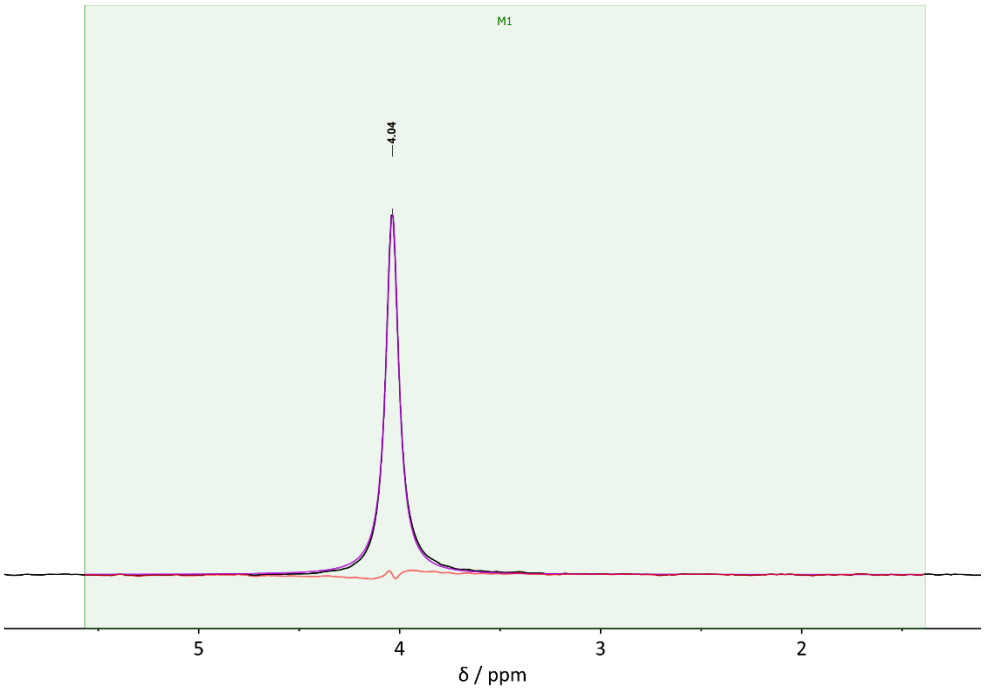

Figure 10: ^{9}Be NMR spectrum of $[BeCl_2(OEt_2)_2]$ (**1a**) in $CDCl_3$ at T = 300 K. Line fitting profiles (purple) and differential plot of calculated *versus* observed line (red) profiles are marked.

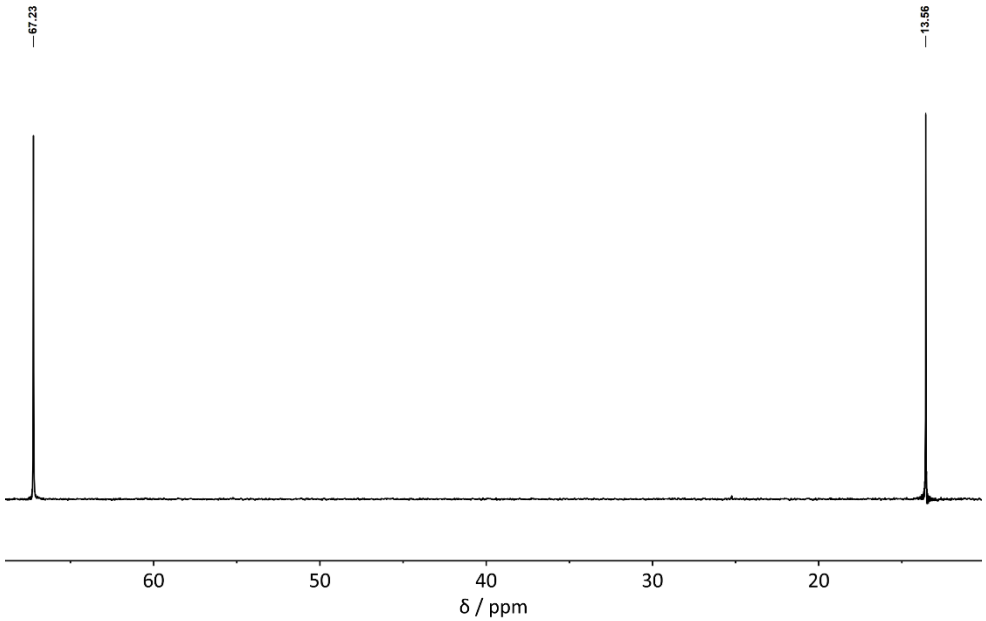

Figure 11: $^{13}C\{^{1}H\}$ NMR spectrum of $[BeCl_2(OEt_2)_2]$ (**1a**) in $CDCl_3$ at T = 300 K.

1.2 $[BeBr_2(OEt_2)_2]$ (1b):

1.2.1 Solvent – Et_2O

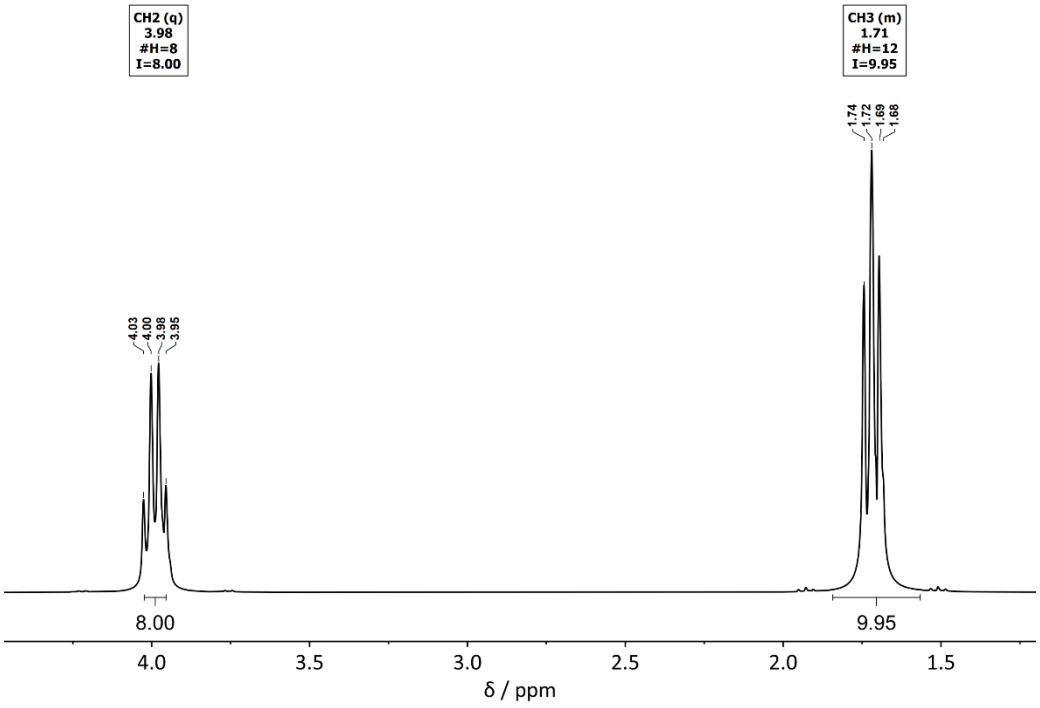

Figure 12: ^{1}H NMR spectrum of $[BeBr_2(OEt_2)_2]$ (**1b**) in Et_2O at T = 300 K.

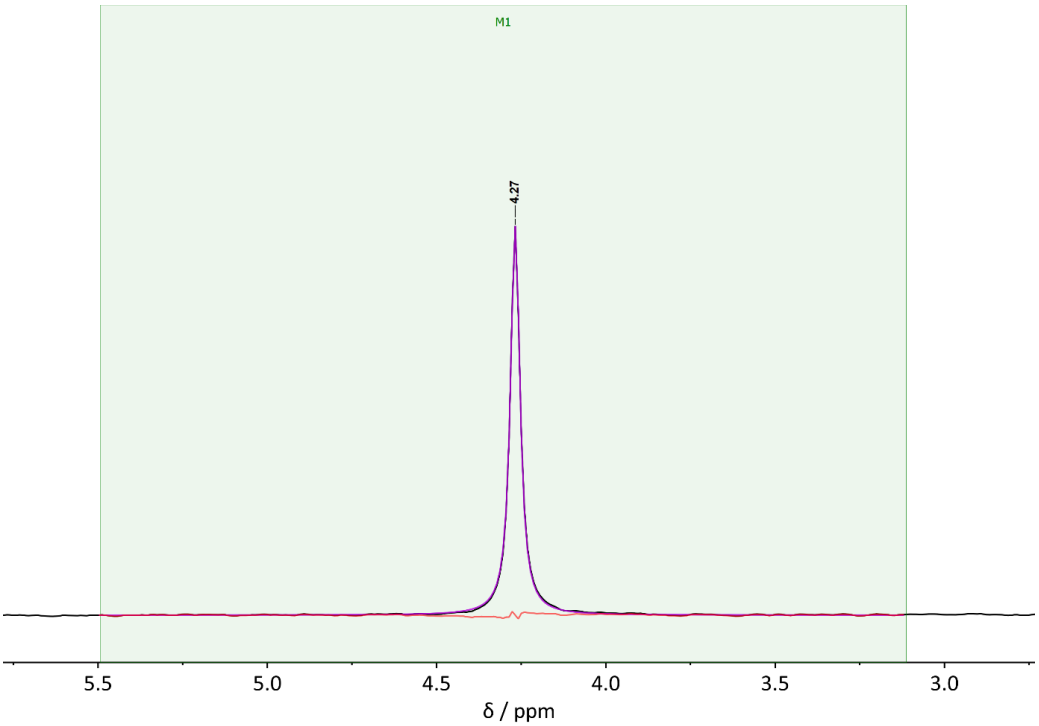

Figure 13: ^{9}Be NMR spectrum of [$BeBr_2(OEt_2)_2$] (**1b**) in Et_2O at *T* = 300 K. Line fitting profiles (purple) and differential plot of calculated *versus* observed line (red) profiles are marked.

1.2.2 Solvent – C_6D_6

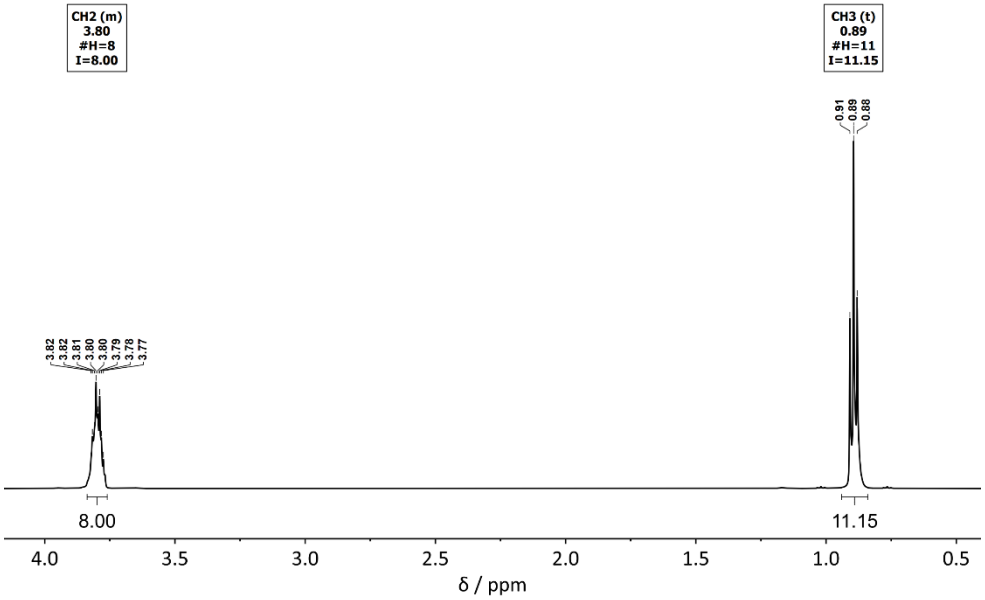

Figure 14: ^{1}H NMR spectrum of [$BeBr_2(OEt_2)_2$] (**1b**) in C_6D_6 at *T* = 300 K.

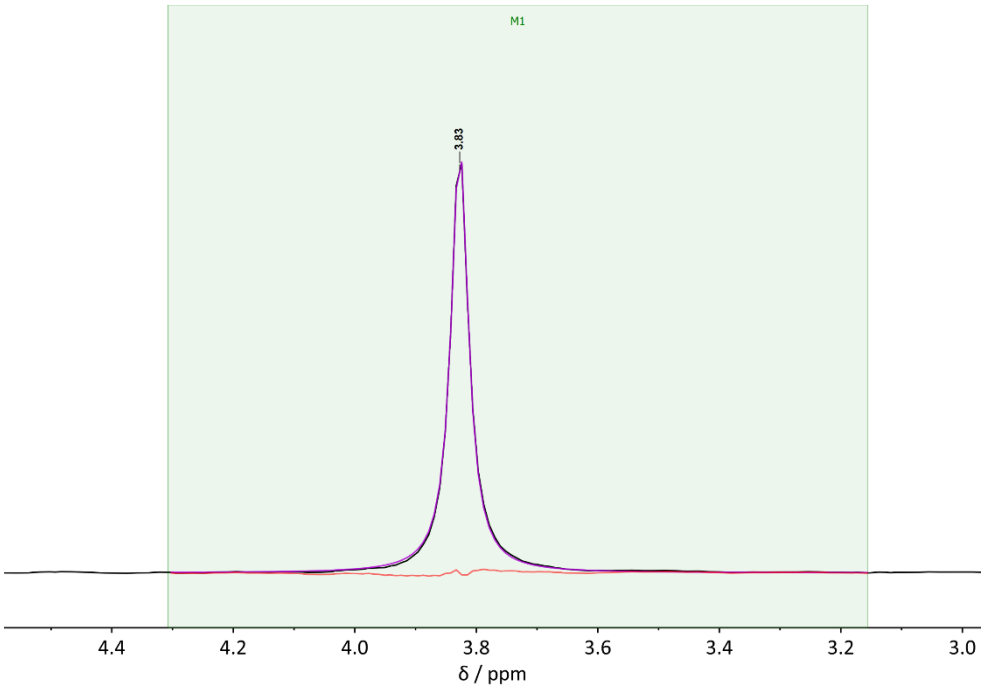

Figure 15: ^{9}Be NMR spectrum of [$BeBr_2(OEt_2)_2$] (**1b**) in C_6D_6 at T = 300 K. Line fitting profiles (purple) and differential plot of calculated *versus* observed line (red) profiles are marked.

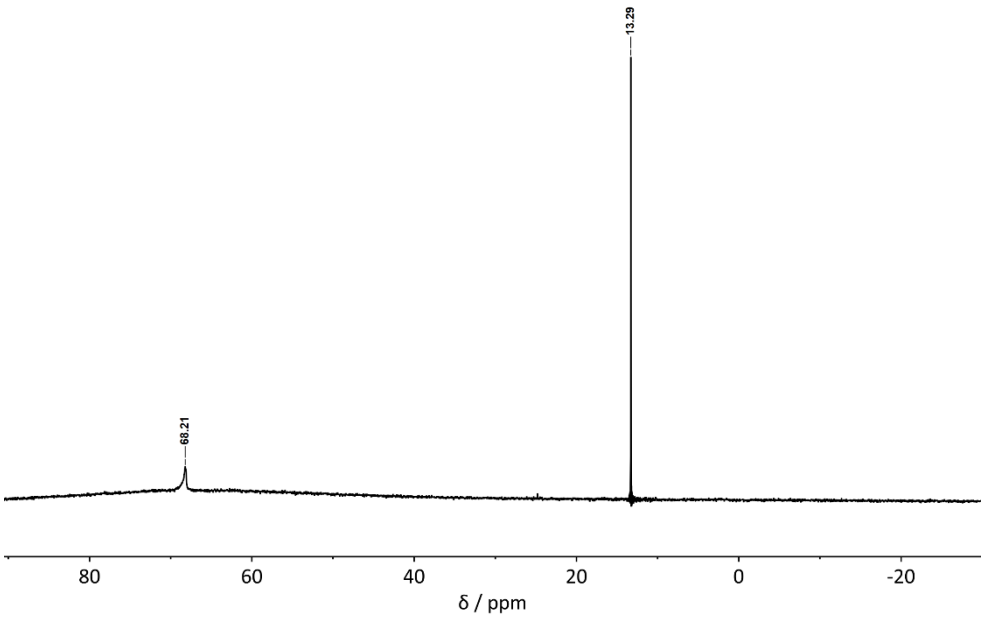

Figure 16: $^{13}C\{^{1}H\}$ NMR spectrum of [$BeBr_2(OEt_2)_2$] (**1b**) in C_6D_6 at T = 300 K.

1.2.3 Solvent – CD_2Cl_2

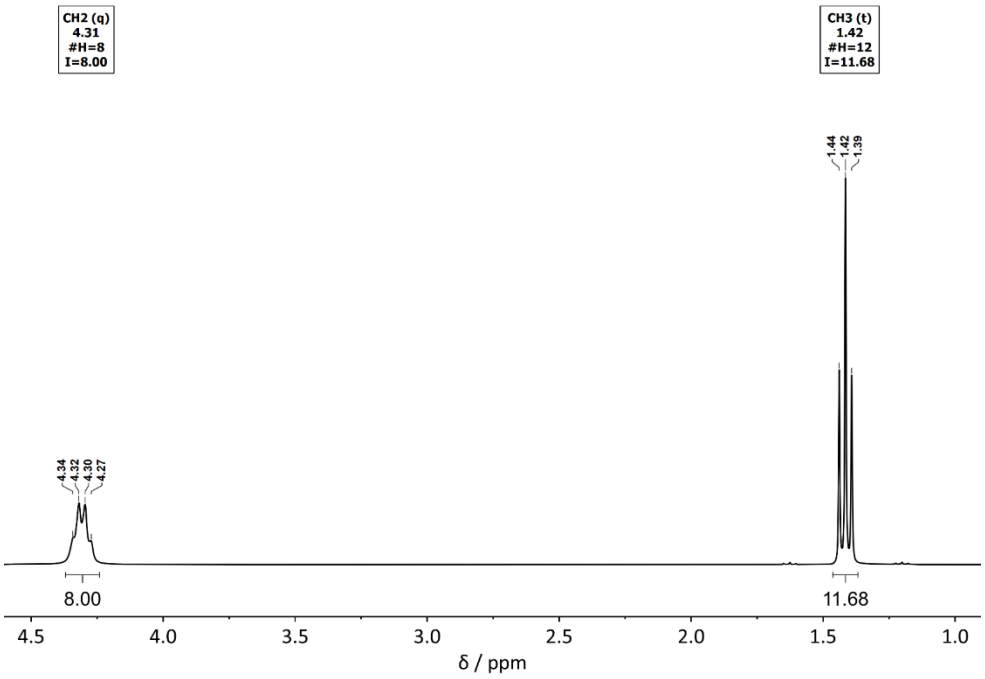

Figure 17: ^{1}H NMR spectrum of [$BeBr_2(OEt_2)_2$] (**1b**) in CD_2Cl_2 at T = 300 K.

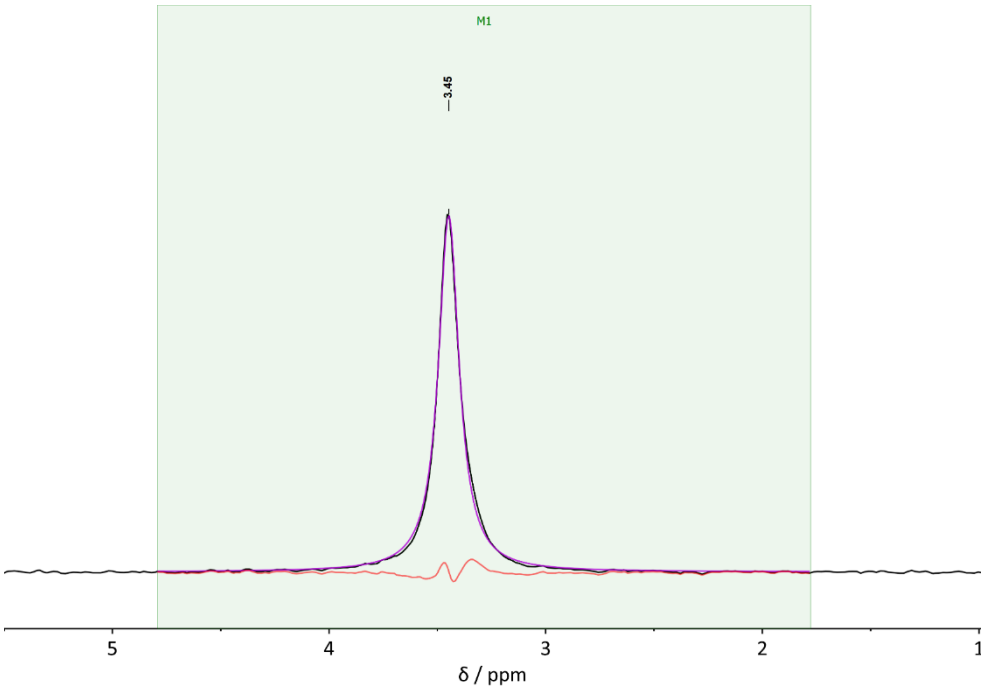

Figure 18: ^{9}Be NMR spectrum of [$BeBr_2(OEt_2)_2$] (**1b**) in CD_2Cl_2 at T = 300 K. Line fitting profiles (purple) and differential plot of calculated *versus* observed line (red) profiles are marked.

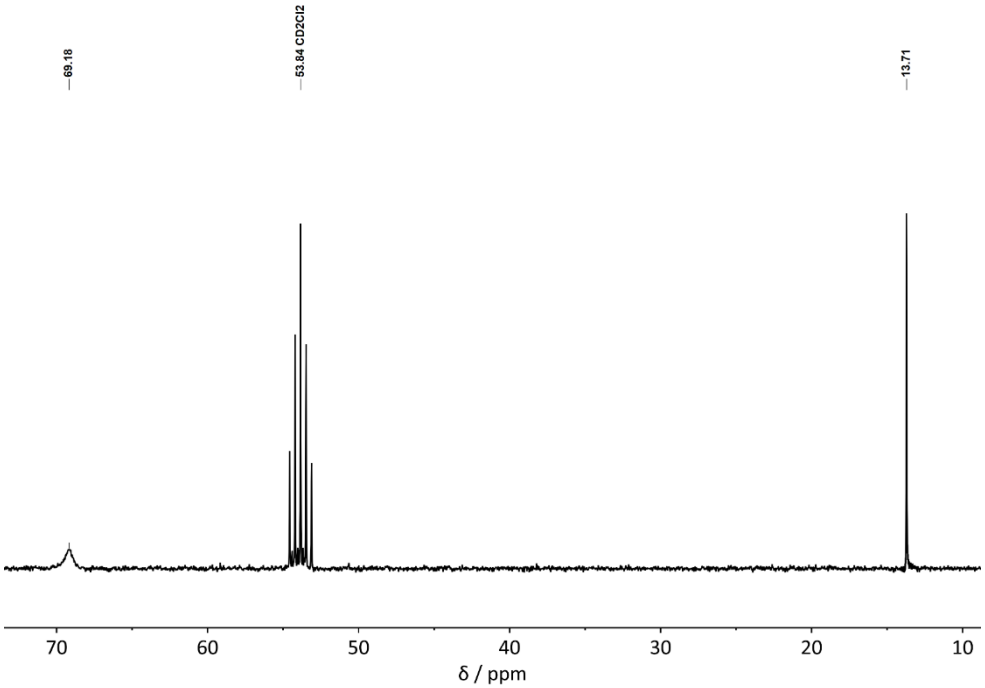

Figure 19: $^{13}C\{^{1}H\}$ NMR spectrum of $[BeBr_2(OEt_2)_2]$ (**1b**) in CD_2Cl_2 at T = 300 K.

1.2.4 Solvent – $CDCl_3$

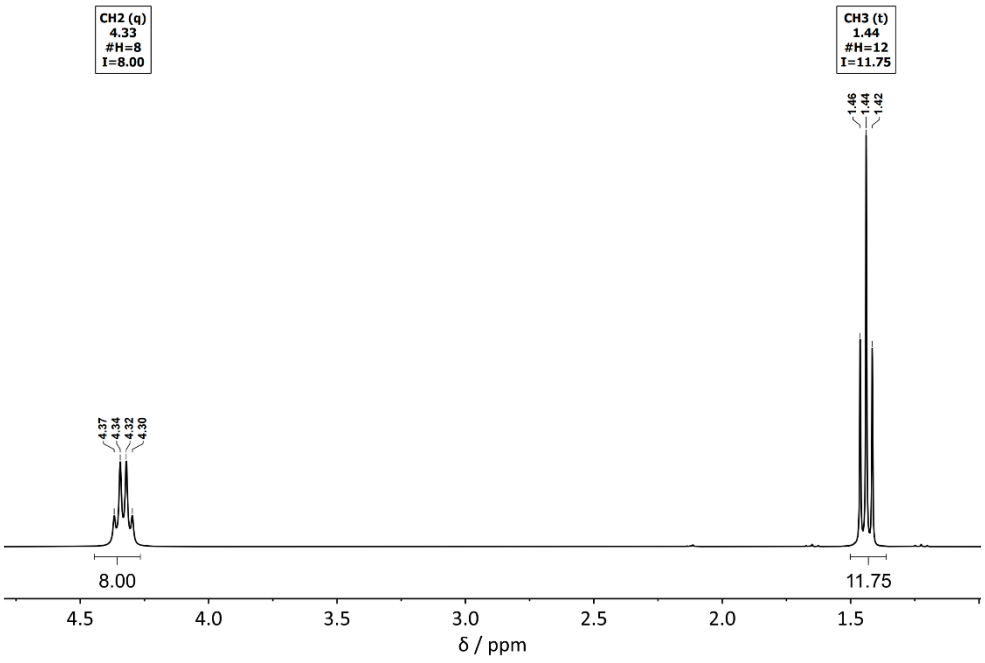

Figure 20: ^{1}H NMR spectrum of $[BeBr_2(OEt_2)_2]$ (**1b**) in $CDCl_3$ at T = 300 K.

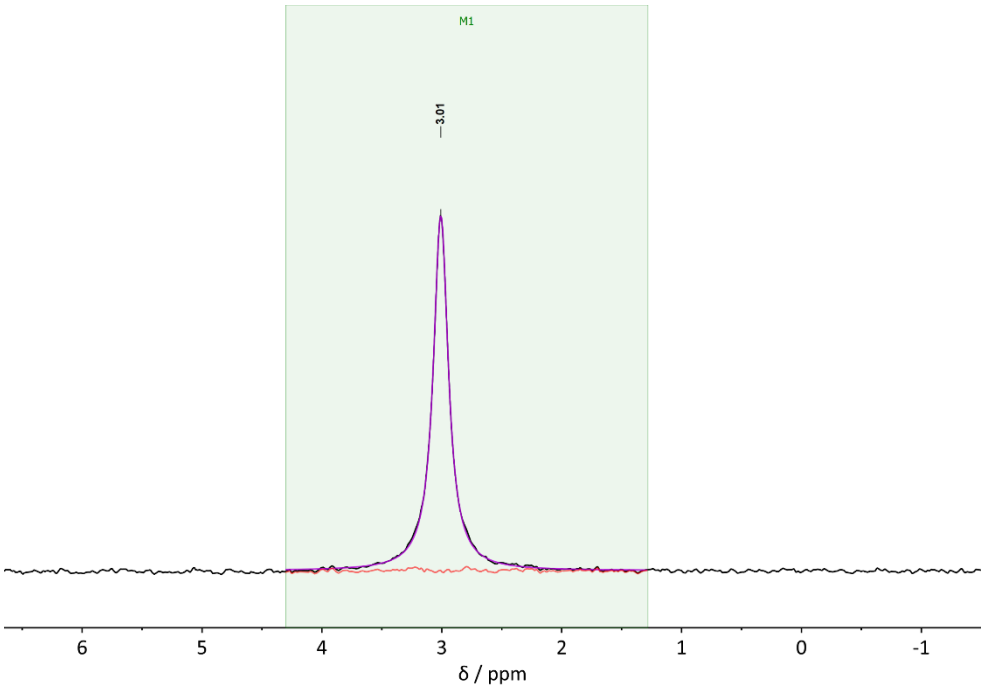

Figure 21: ^{9}Be NMR spectrum of [$BeBr_2(OEt_2)_2$] (**1b**) in $CDCl_3$ at *T* = 300 K. Line fitting profiles (purple) and differential plot of calculated *versus* observed line (red) profiles are marked.

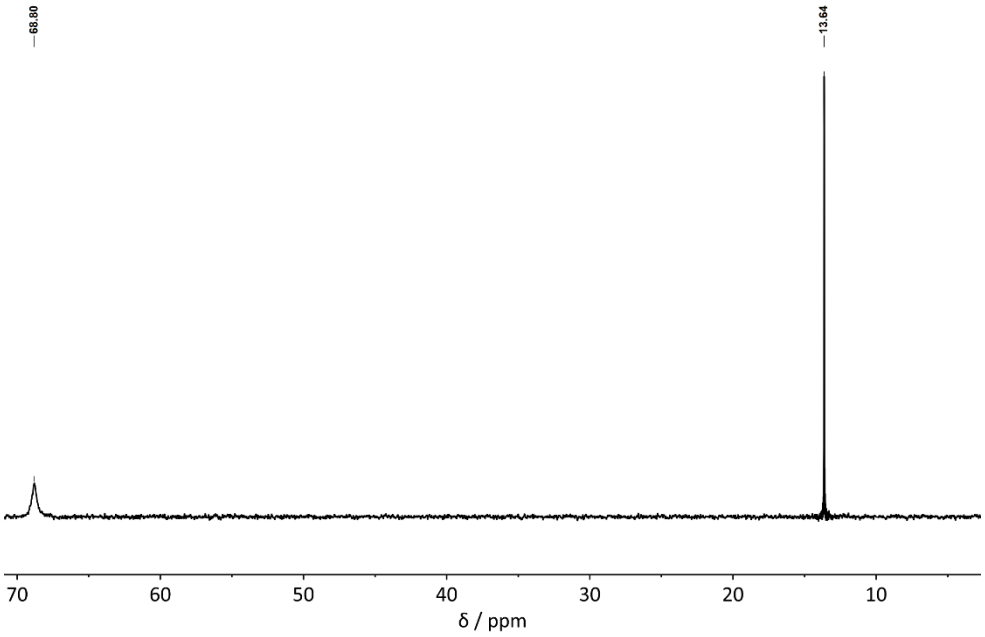

Figure 22: $^{13}C\{^{1}H\}$ NMR spectrum of [$BeBr_2(OEt_2)_2$] (**1b**) in $CDCl_3$ at *T* = 300 K.

1.3 $[BeI_2(OEt_2)_2]$ (1c):

1.3.1 Solvent – Et_2O

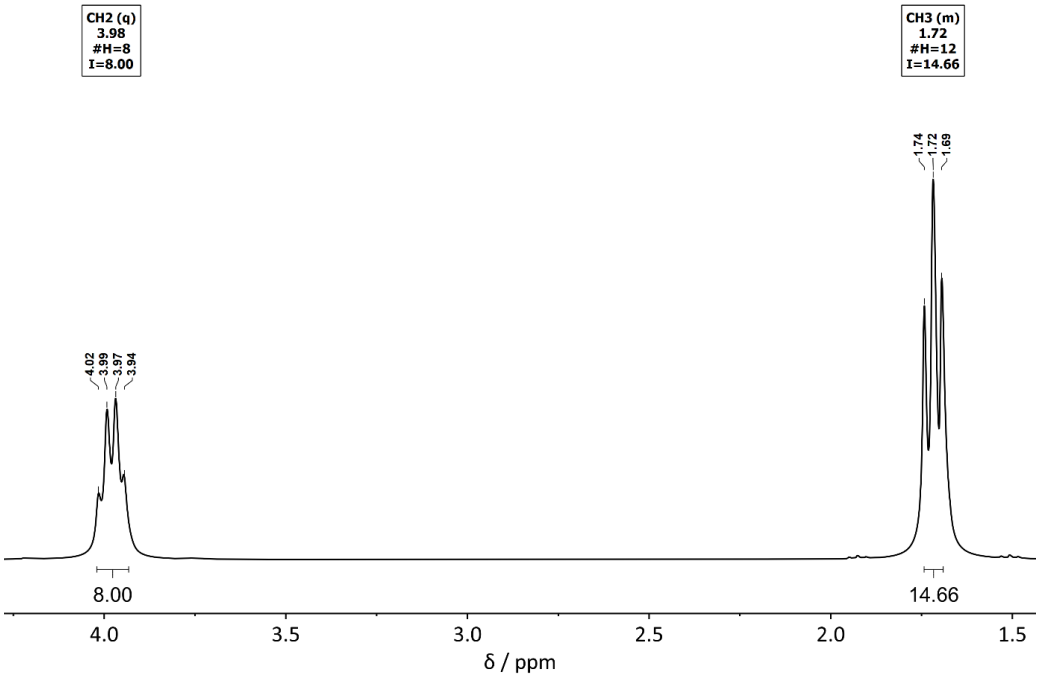

Figure 23: ^{1}H NMR spectrum of $[BeI_2(OEt_2)_2]$ (**1c**) in Et_2O at T = 300 K.

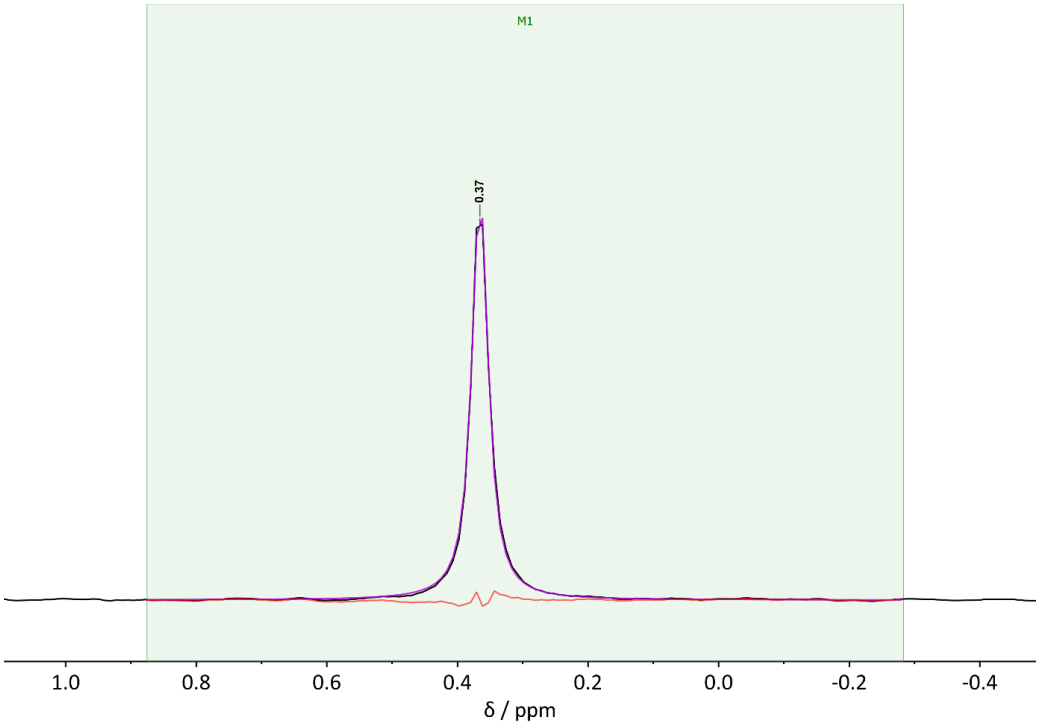

Figure 24: ^{9}Be NMR spectrum of $[BeI_2(OEt_2)_2]$ (**1c**) in Et_2O at T = 300 K. Line fitting profiles (purple) and differential plot of calculated *versus* observed line (red) profiles are marked.

1.3.2 Solvent – C_6D_6

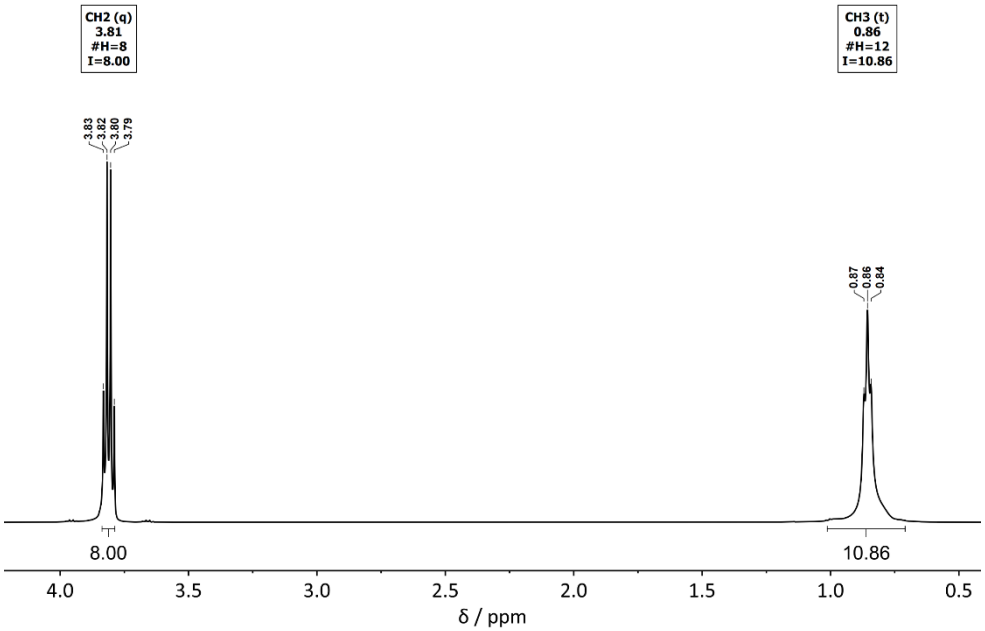

Figure 25: ^{1}H NMR spectrum of $[BeI_2(OEt_2)_2]$ (**1c**) in C_6D_6 at T = 300 K.

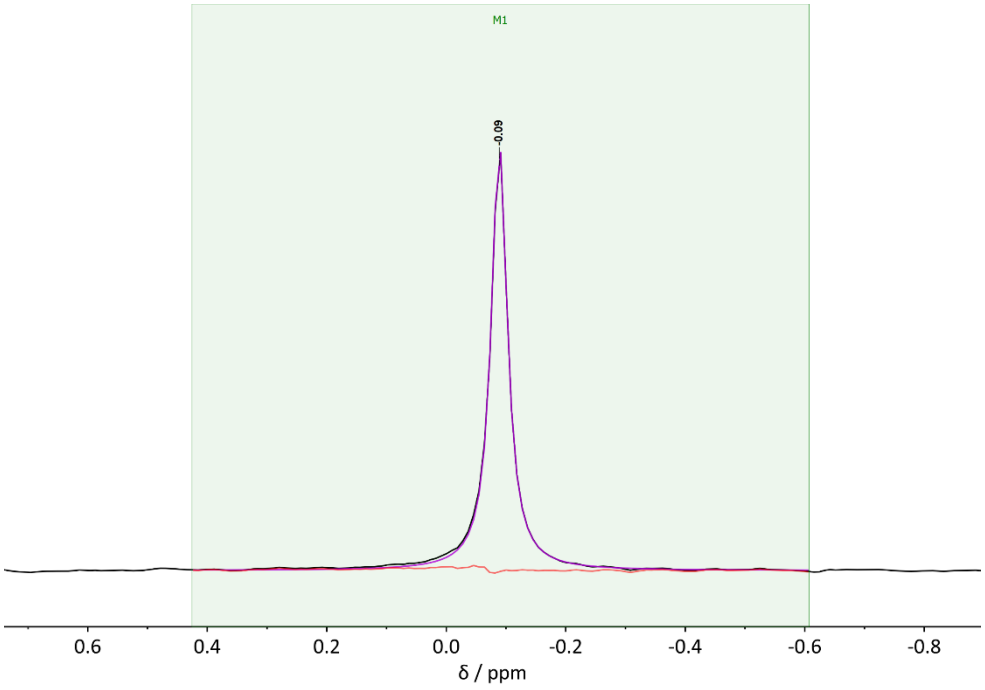

Figure 26: ^{9}Be NMR spectrum of $[BeI_2(OEt_2)_2]$ (**1c**) in C_6D_6 at T = 300 K. Line fitting profiles (purple) and differential plot of calculated *versus* observed line (red) profiles are marked.

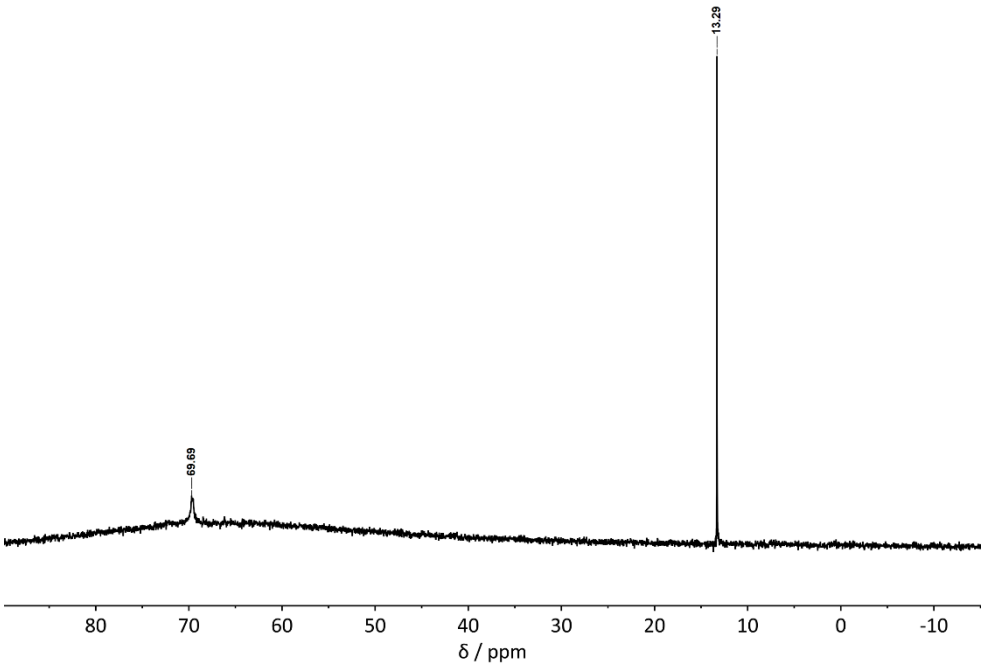

Figure 27: $^{13}C\{^{1}H\}$ NMR spectrum of $[BeI_2(OEt_2)_2]$ (**1c**) in C_6D_6 at T = 300 K.

1.3.3 Solvent – CD_2Cl_2

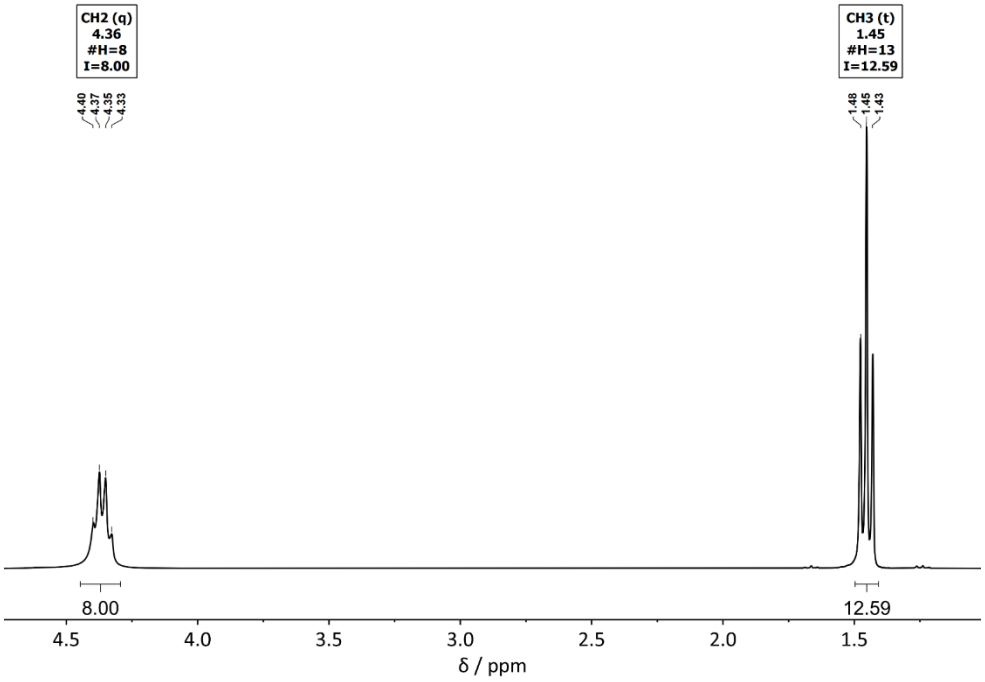

Figure 28: ^{1}H NMR spectrum of $[BeI_2(OEt_2)_2]$ (**1c**) in CD_2Cl_2 at T = 300 K.

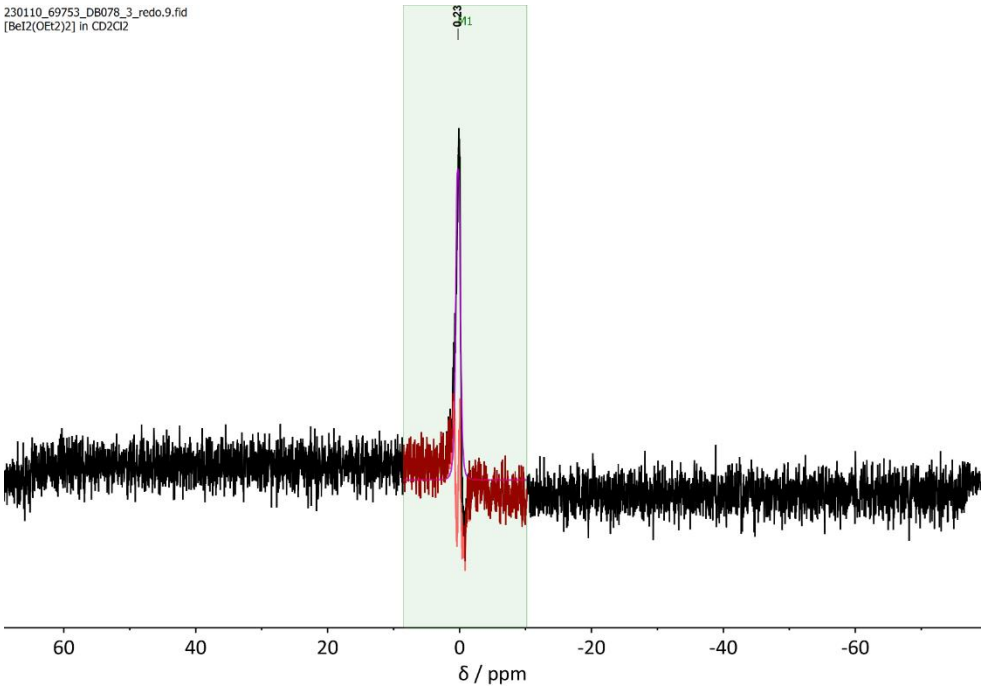

Figure 29: ^{9}Be NMR spectrum of [$BeI_2(OEt_2)_2$] (**1c**) in CD_2Cl_2 at *T* = 300 K. Line fitting profiles (purple) and differential plot of calculated *versus* observed line (red) profiles are marked.

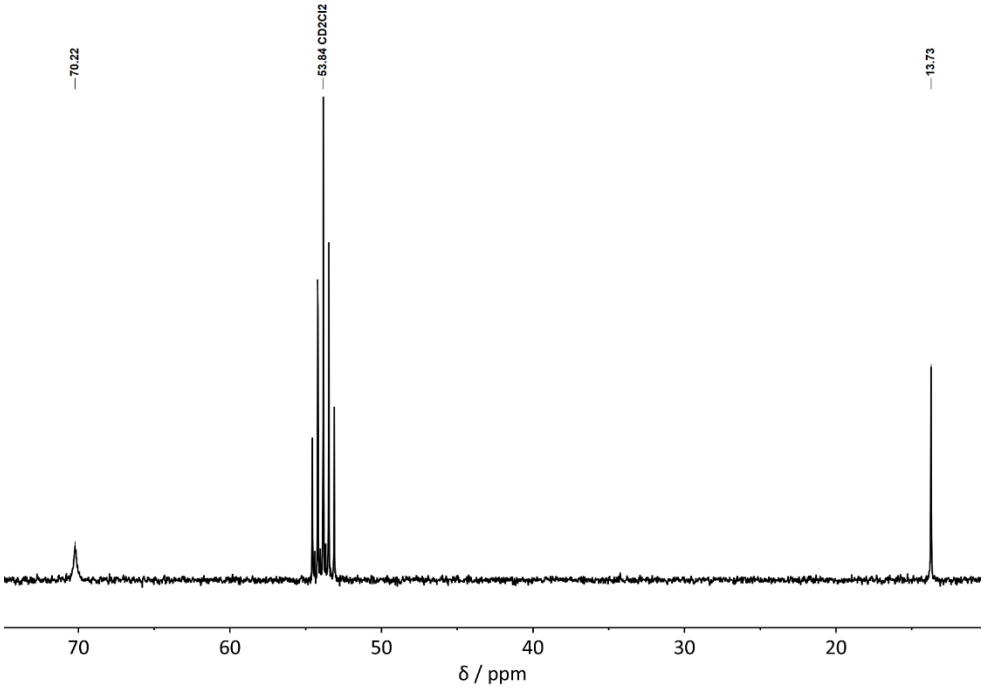

Figure 30: $^{13}C\{^{1}H\}$ NMR spectrum of [$BeI_2(OEt_2)_2$] (**1c**) in CD_2Cl_2 at *T* = 300 K.

1.3.4 Solvent – $CDCl_3$

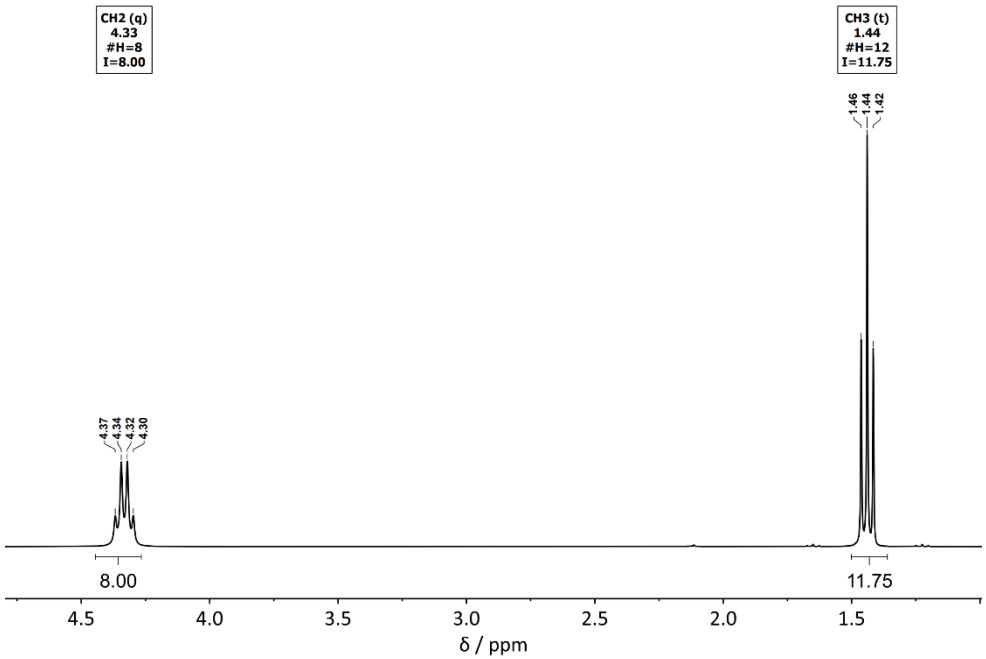

Figure 31: ^{1}H NMR spectrum of $[BeI_2(OEt_2)_2]$ (**1c**) in $CDCl_3$ at T = 300 K.

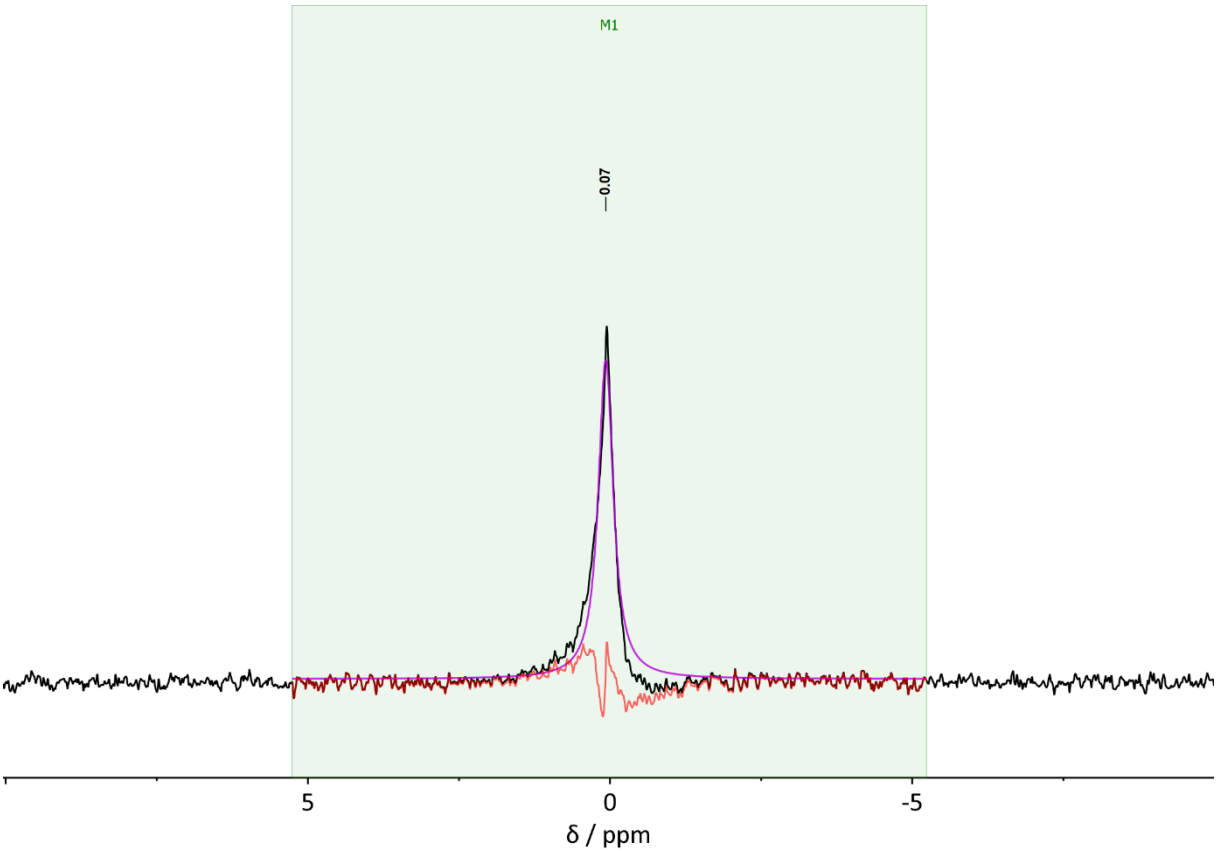

Figure 32: ^{9}Be NMR spectrum of $[BeI_2(OEt_2)_2]$ (**1c**) in $CDCl_3$ at T = 300 K. Line fitting profiles (purple) and differential plot of calculated *versus* observed line (red) profiles are marked.

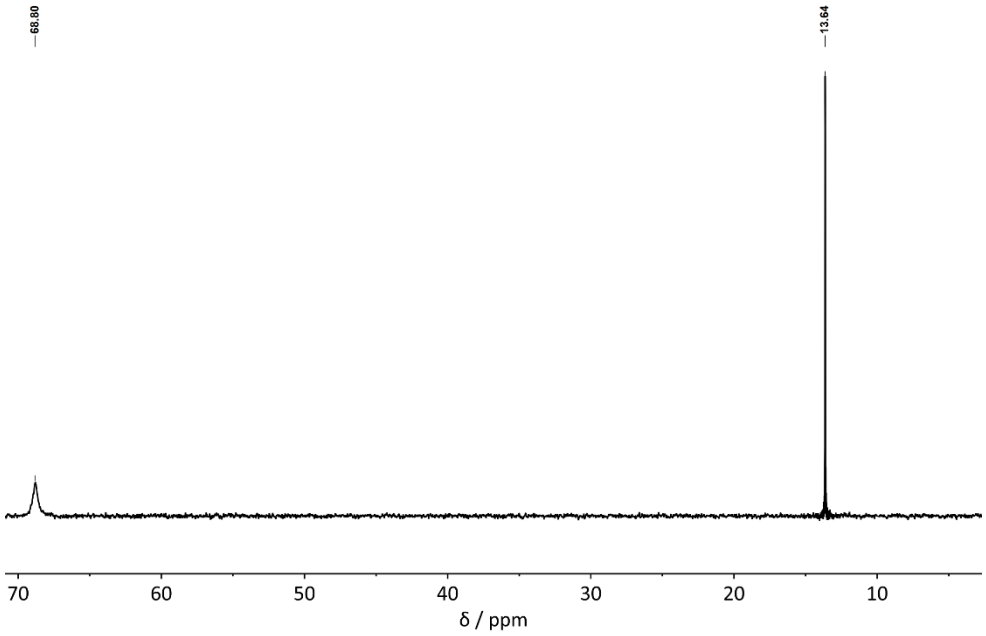

Figure 33: $^{13}C\{^{1}H\}$ NMR spectrum of $[BeI_2(OEt_2)_2]$ (**1c**) in $CDCl_3$ at T = 300 K.

1.4 $[BeCl_2(thf)_2]$ (2a):

1.4.1 Solvent – thf-*d8*

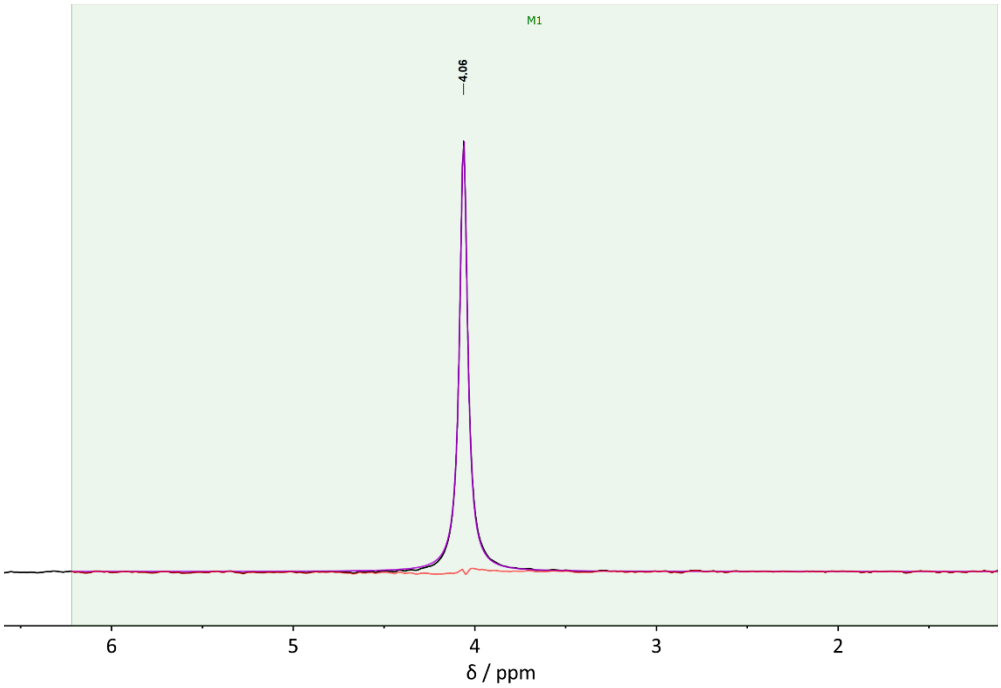

Figure 34: ^{9}Be NMR spectrum of $[BeCl_2(thf)_2]$ (**2a**) in thf-*d8* at T = 300 K. Line fitting profiles (purple) and differential plot of calculated *versus* observed line (red) profiles are marked.

1.4.2 Solvent – C_6D_6

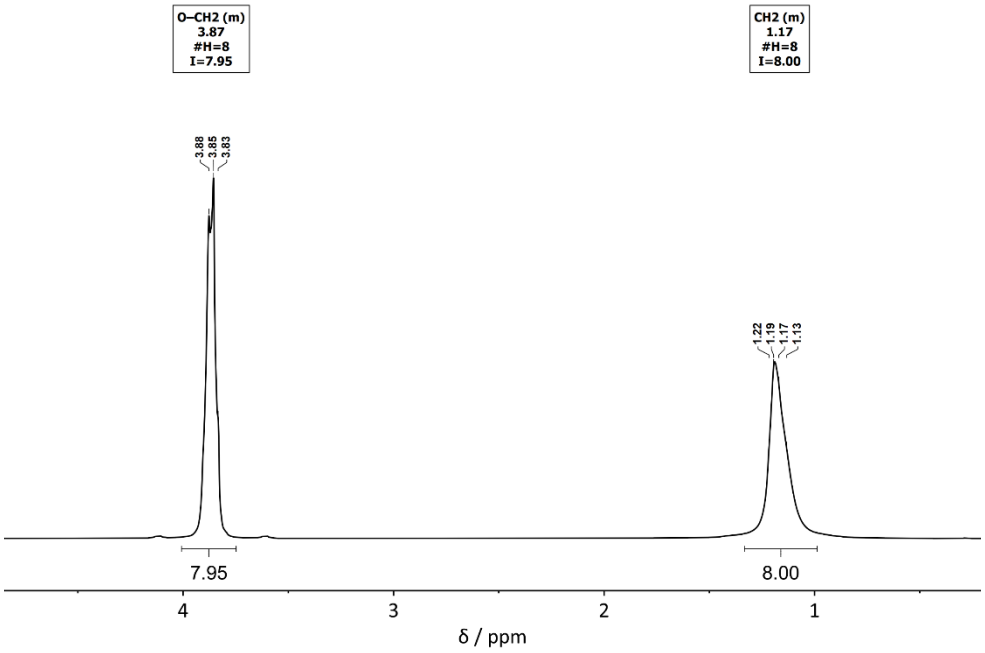

Figure 35: ^{1}H NMR spectrum of $[BeCl_2(thf)_2]$ (**2a**) in C_6D_6 at T = 300 K.

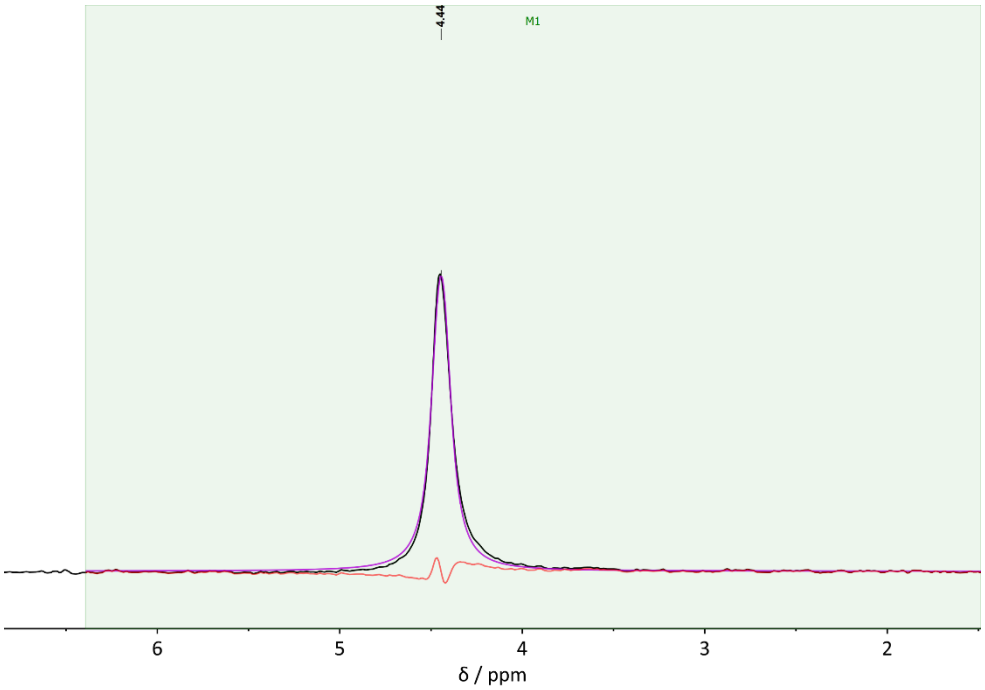

Figure 36: ^{9}Be NMR spectrum of $[BeCl_2(thf)_2]$ (**2a**) in C_6D_6 at T = 300 K. Line fitting profiles (purple) and differential plot of calculated *versus* observed line (red) profiles are marked.

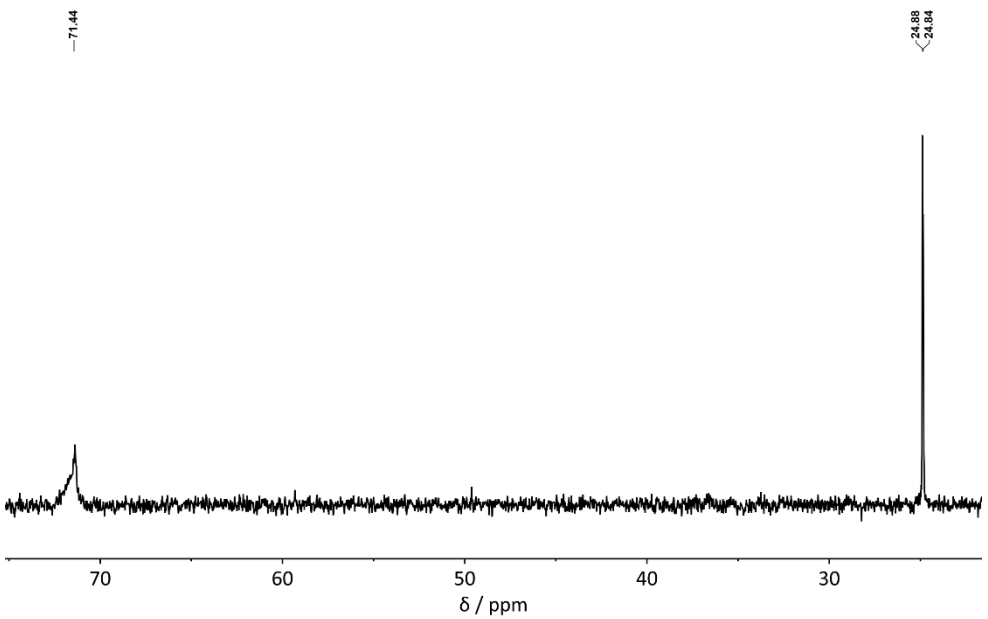

Figure 37: $^{13}C\{^{1}H\}$ NMR spectrum of $[BeCl_2(thf)_2]$ (**2a**) in C_6D_6 at T = 300 K.

1.4.3 Solvent – CD_2Cl_2

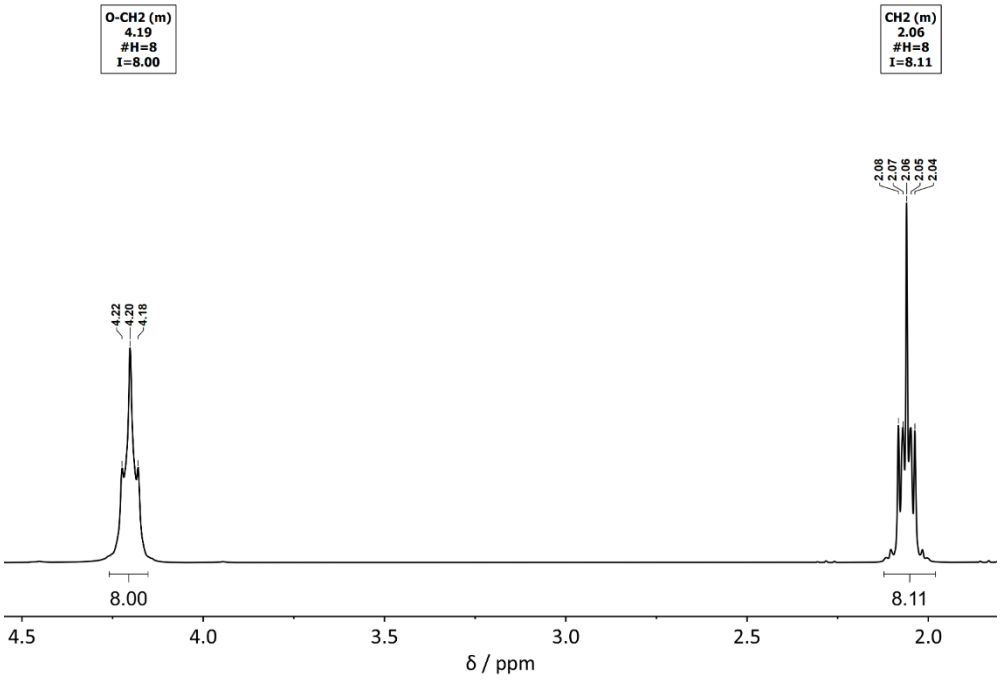

Figure 38: ^{1}H NMR spectrum of $[BeCl_2(thf)_2]$ (**2a**) in CD_2Cl_2 at T = 300 K.

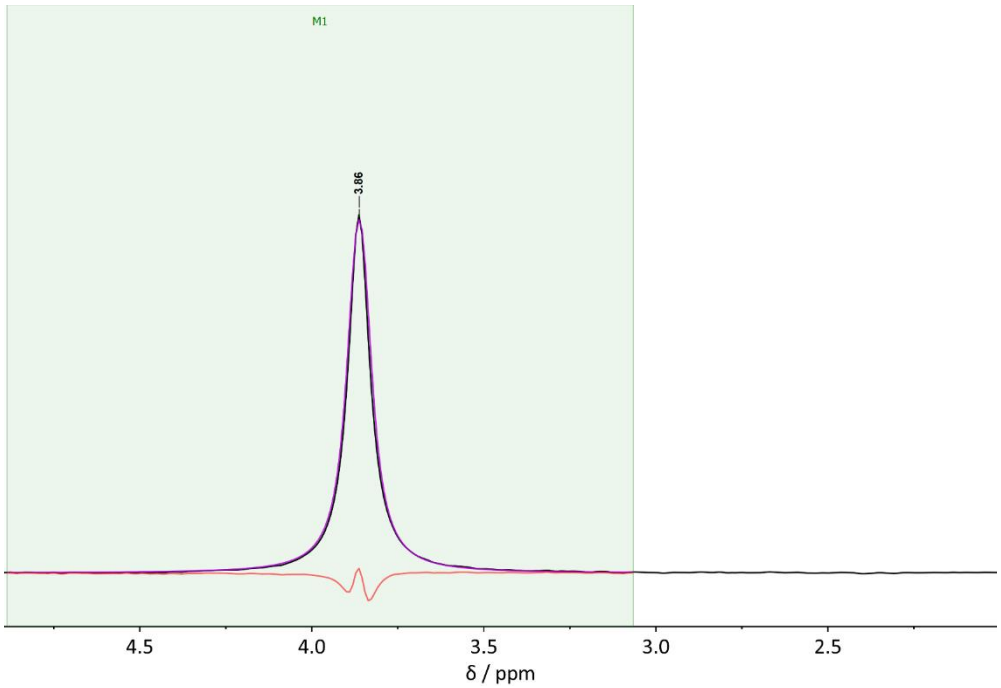

Figure 39: ^{9}Be NMR spectrum of [$BeCl_2(thf)_2$] (**2a**) in CD_2Cl_2 at T = 300 K. Line fitting profiles (purple) and differential plot of calculated *versus* observed line (red) profiles are marked.

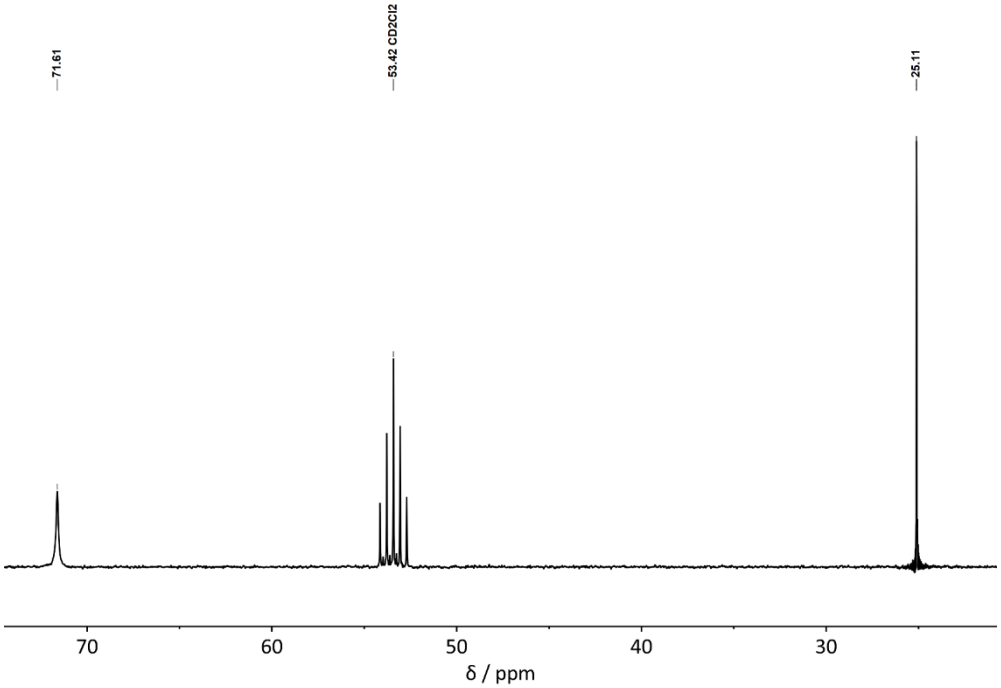

Figure 40: $^{13}C\{^{1}H\}$ NMR spectrum of [$BeCl_2(thf)_2$] (**2a**) in CD_2Cl_2 at T = 300 K.

1.4.4 Solvent – $CDCl_3$

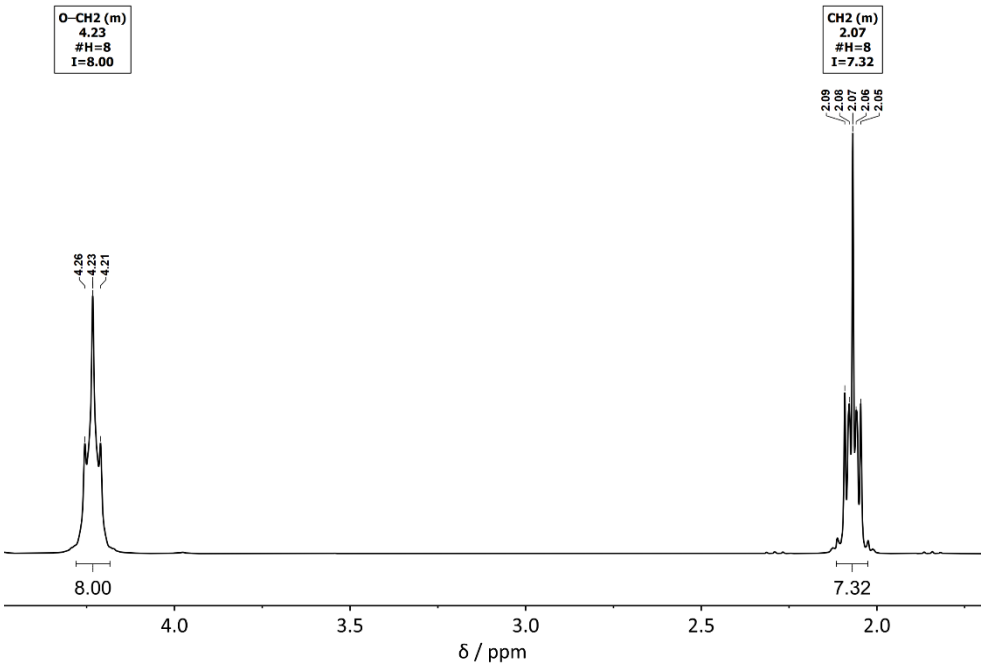

Figure 41: ^{1}H NMR spectrum of $[BeCl_2(thf)_2]$ (**2a**) in $CDCl_3$ at T = 300 K.

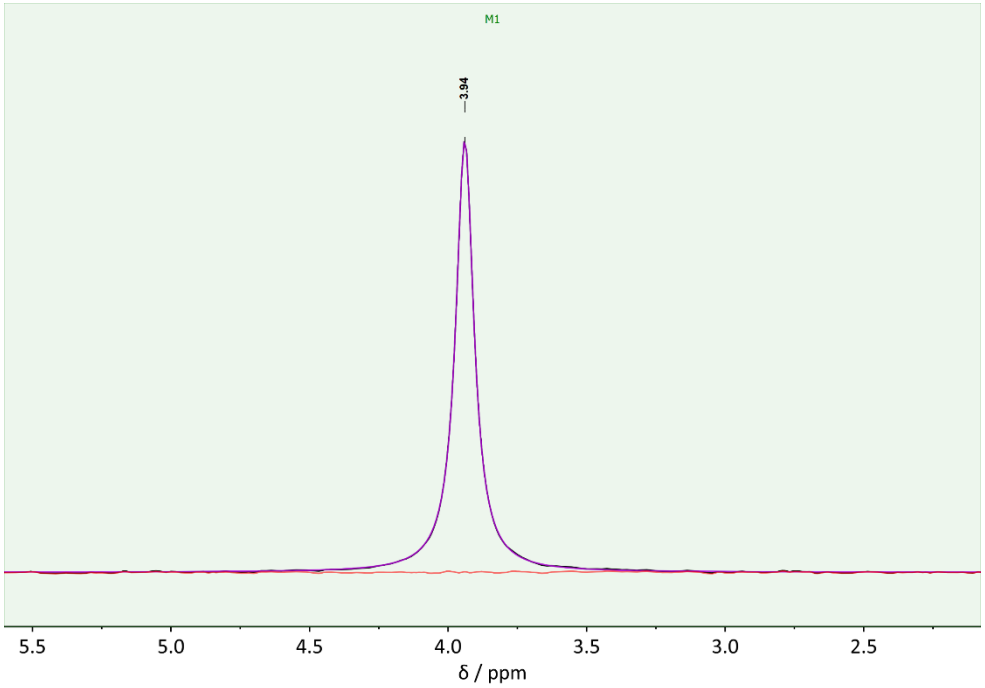

Figure 42: ^{9}Be NMR spectrum of $[BeCl_2(thf)_2]$ (**2a**) in $CDCl_3$ at T = 300 K. Line fitting profiles (purple) and differential plot of calculated *versus* observed line (red) profiles are marked.

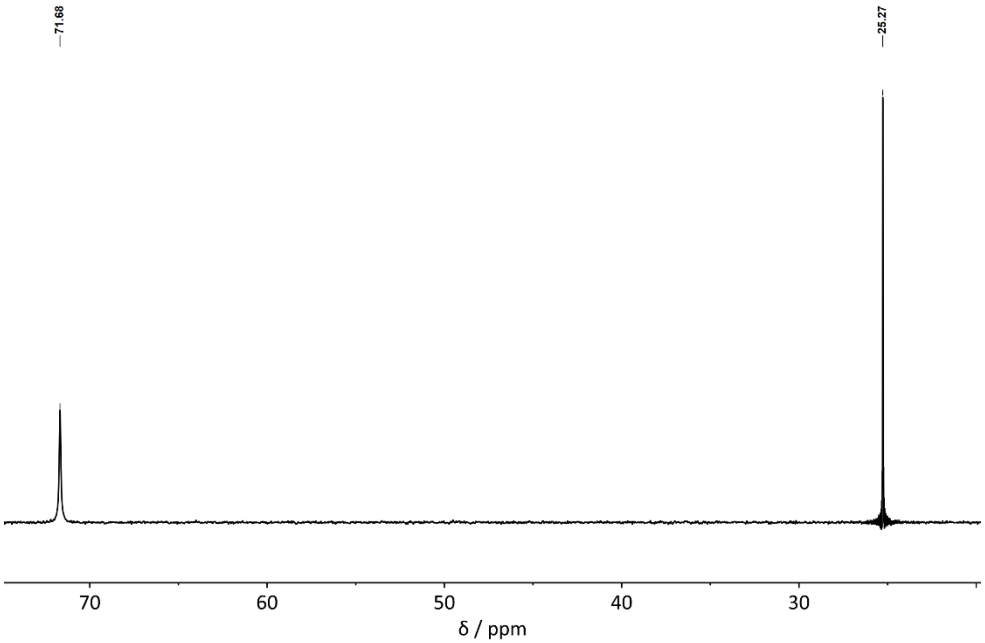

Figure 43: ^{13}C NMR spectrum of $[BeCl_2(thf)_2]$ (**2a**) in $CDCl_3$ at T = 300 K.

1.5 $[BeBr_2(thf)_2]$ (2b):

1.5.1 Solvent – thf-*d8*

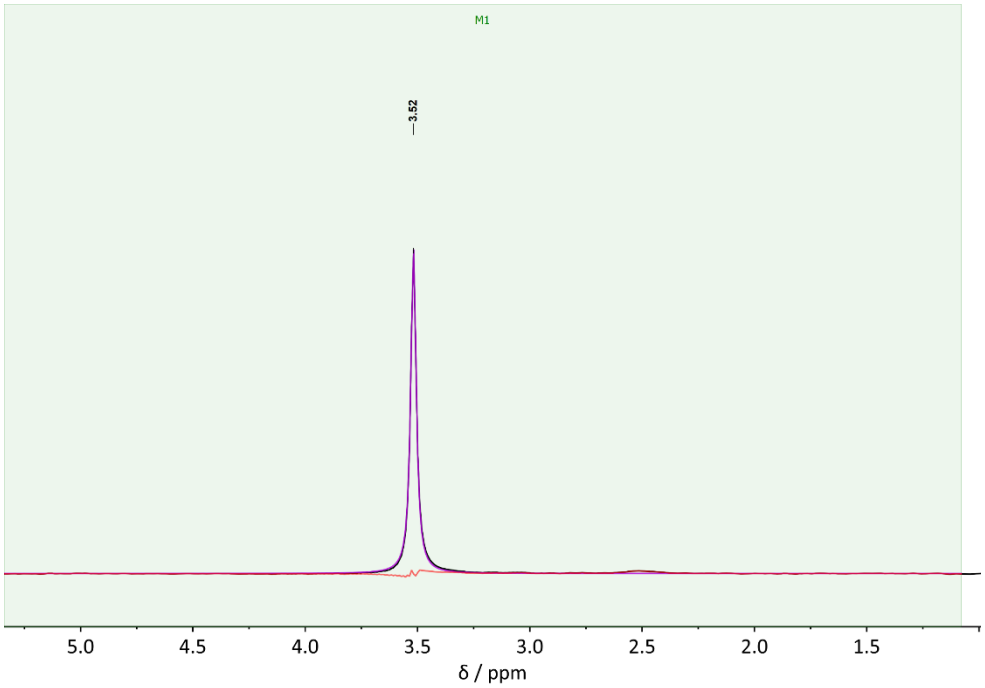

Figure 44: ^{9}Be NMR spectrum of $[BeBr_2(thf)_2]$ (**2b**) in thf-*d8* at T = 300 K. Line fitting profiles (purple) and differential plot of calculated *versus* observed line (red) profiles are marked.

1.5.2 Solvent – C_6D_6

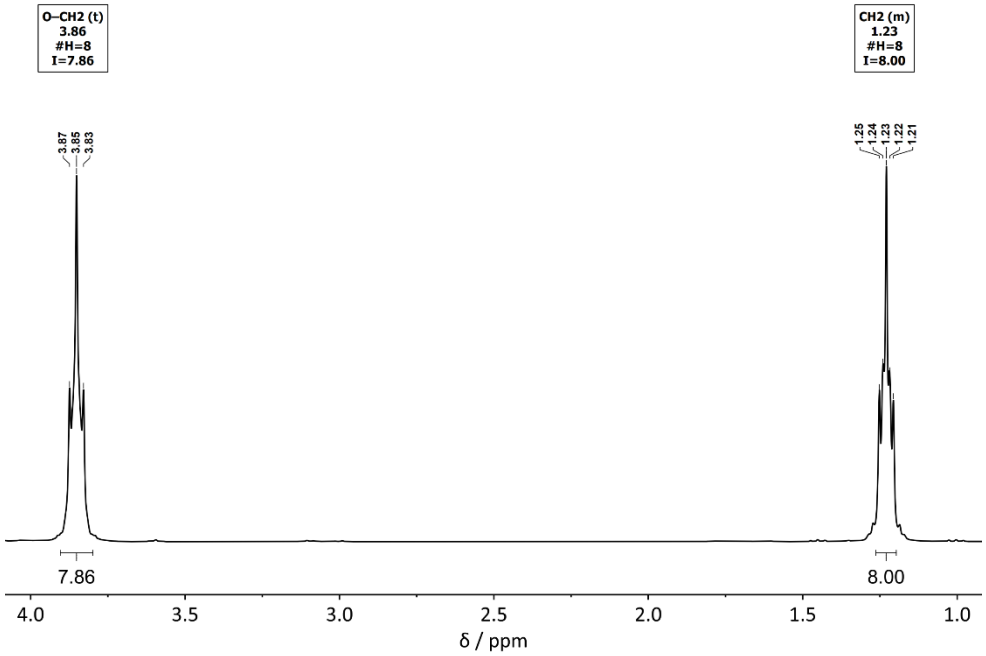

Figure 45: ^{1}H NMR spectrum of [$BeBr_2(thf)_2$] (**2b**) in C_6D_6 at T = 300 K.

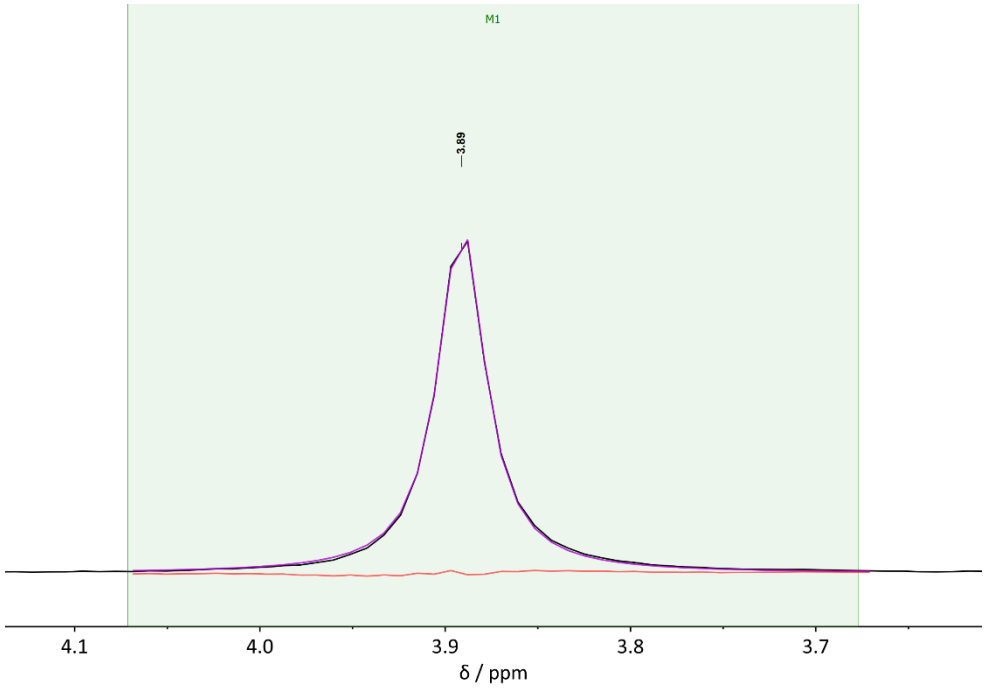

Figure 46: ^{9}Be NMR spectrum of [$BeBr_2(thf)_2$] (**2b**) in C_6D_6 at T = 300 K. Line fitting profiles (purple) and differential plot of calculated *versus* observed line (red) profiles are marked.

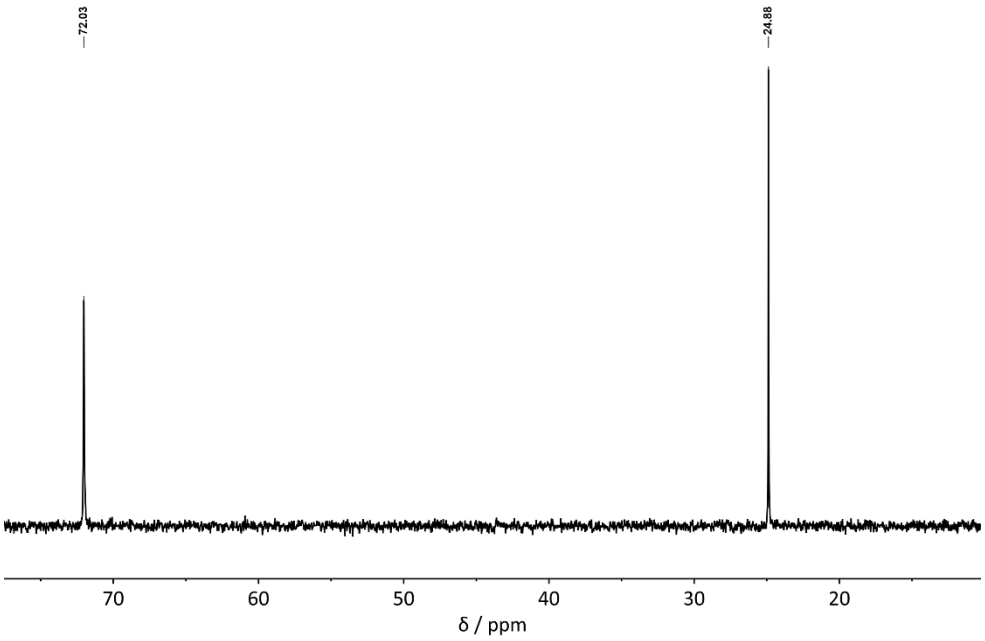

Figure 47: $^{13}C\{^{1}H\}$ NMR spectrum of $[BeBr_2(thf)_2]$ (**2b**) in C_6D_6 at T = 300 K.

1.5.3 Solvent – CD_2Cl_2

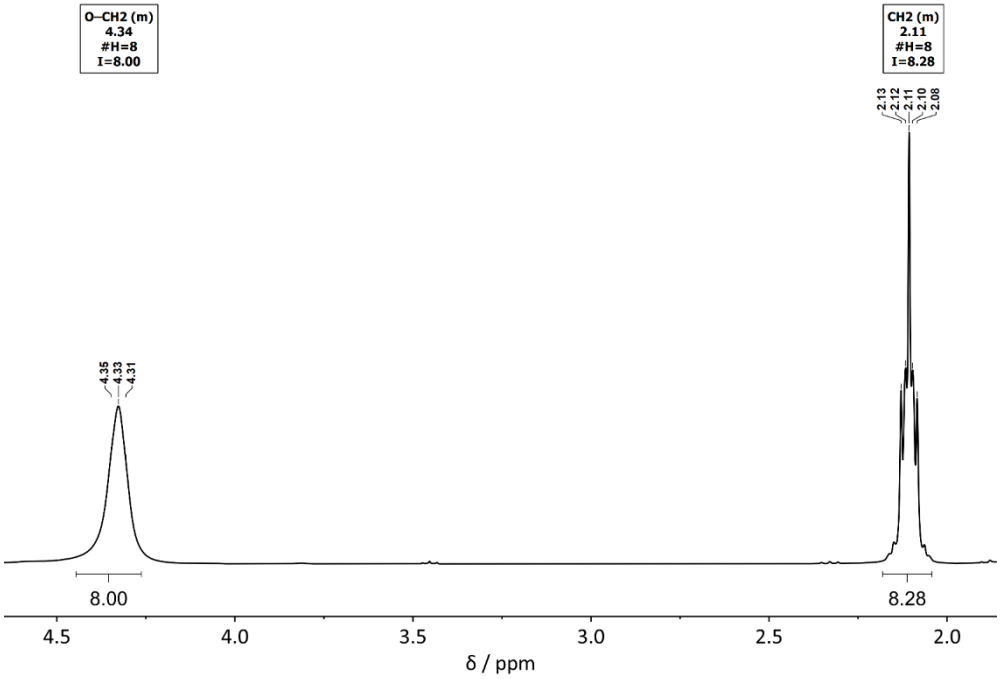

Figure 48: ^{1}H NMR spectrum of $[BeBr_2(thf)_2]$ (**2b**) in CD_2Cl_2 at T = 300 K.

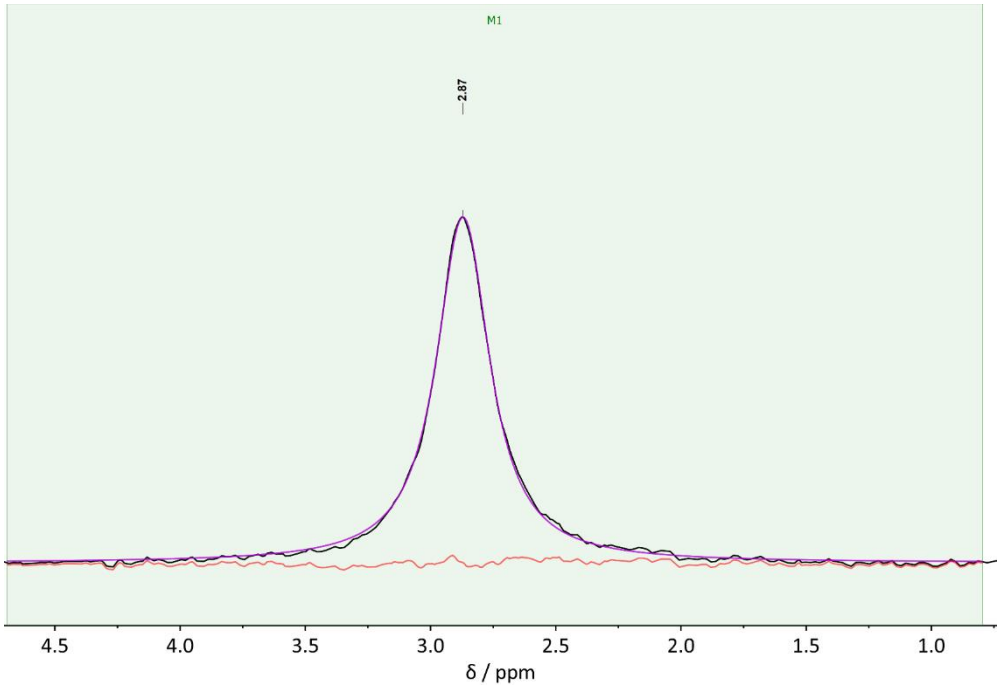

Figure 49: ^{9}Be NMR spectrum of [$BeBr_2(thf)_2$] (**2b**) in CD_2Cl_2 at *T* = 300 K. Line fitting profiles (purple) and differential plot of calculated *versus* observed line (red) profiles are marked.

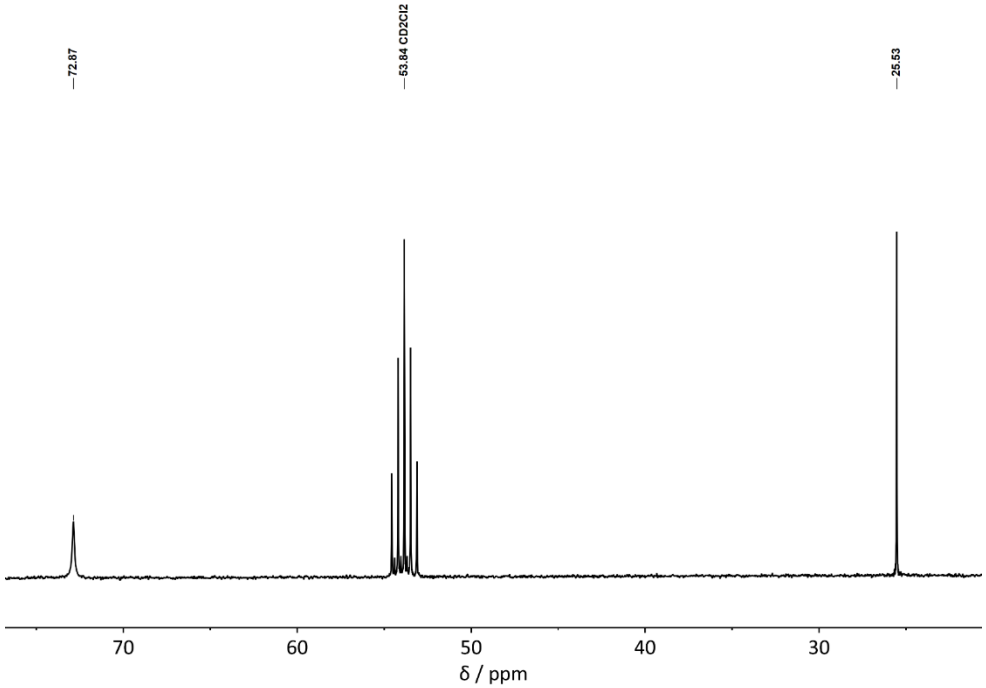

Figure 50: $^{13}C\{^{1}H\}$ NMR spectrum of [$BeBr_2(thf)_2$] (**2b**) in CD_2Cl_2 at *T* = 300 K.

1.5.4 Solvent – $CDCl_3$

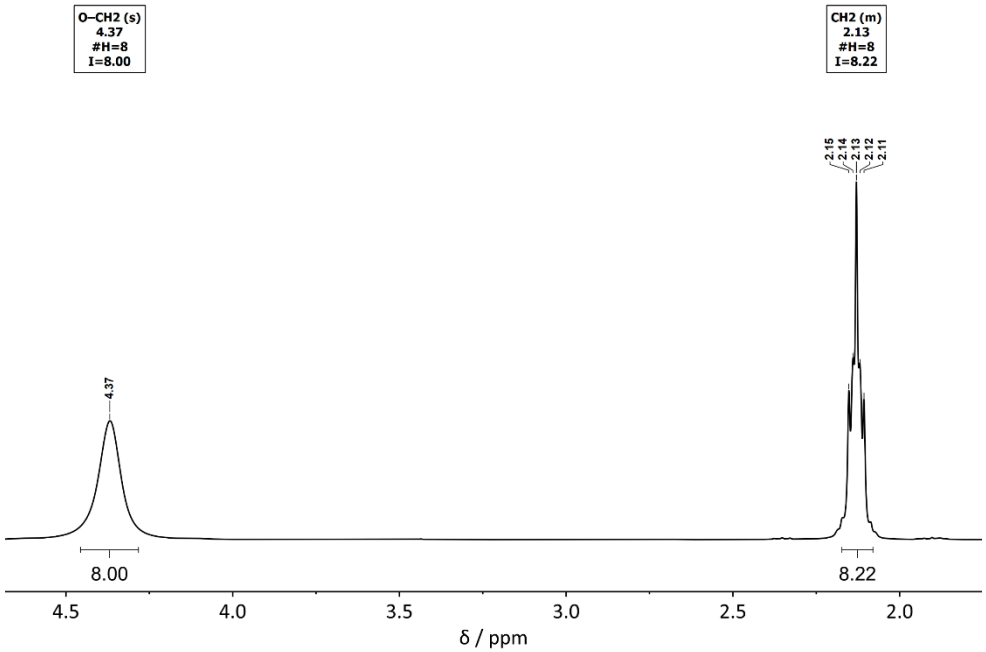

Figure 51: ^{1}H NMR spectrum of [$BeBr_2(thf)_2$] (**2b**) in $CDCl_3$ at T = 300 K.

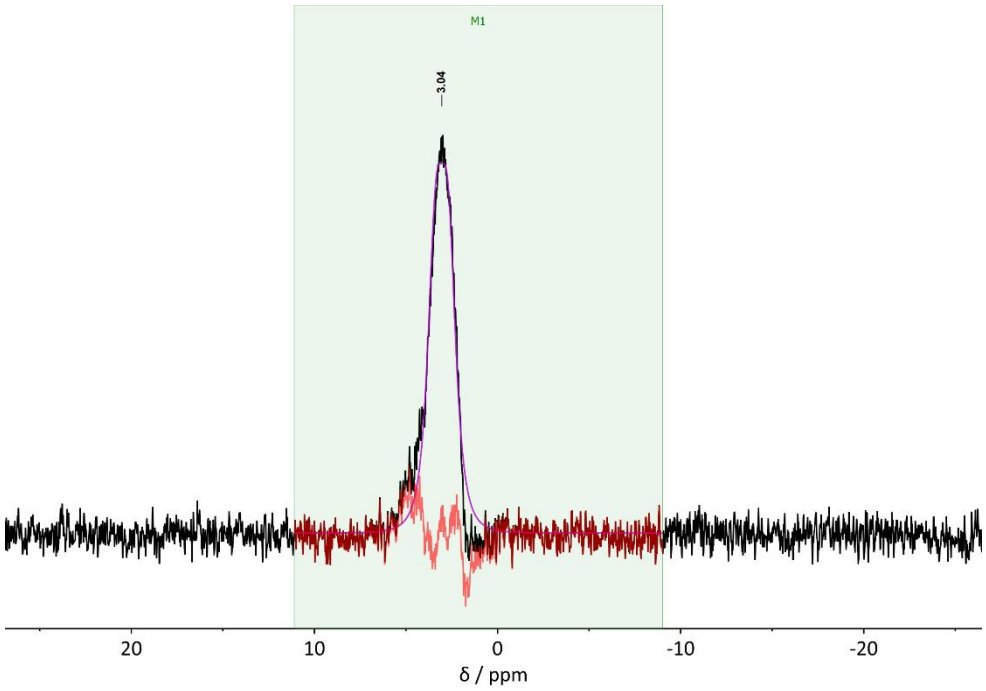

Figure 52: ^{9}Be NMR spectrum of [$BeBr_2(thf)_2$] (**2b**) in $CDCl_3$ at T = 300 K. Line fitting profiles (purple) and differential plot of calculated *versus* observed line (red) profiles are marked.

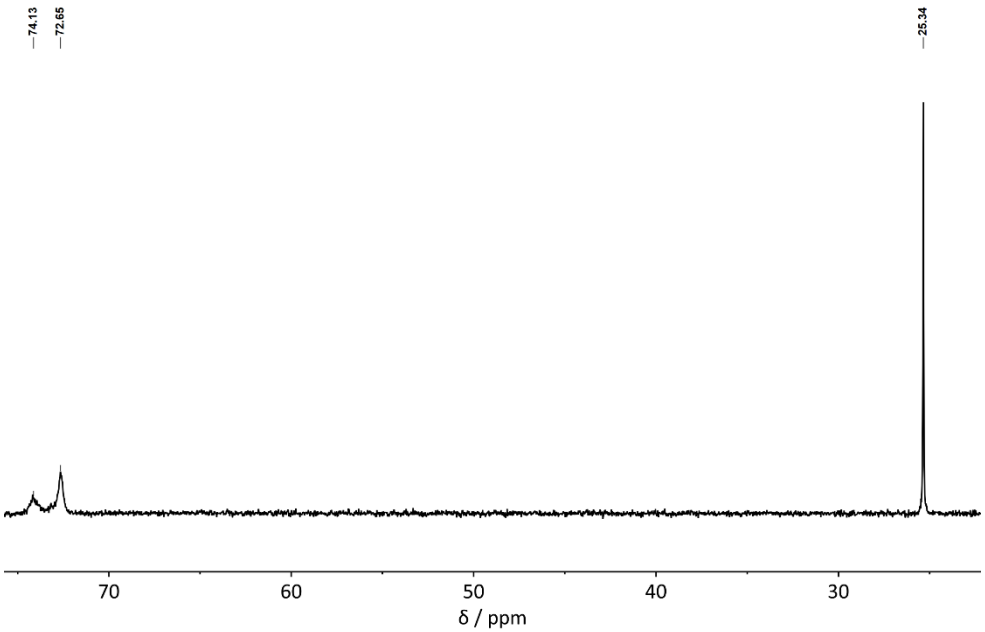

Figure 53: $^{13}C\{^{1}H\}$ NMR spectrum of $[BeBr_2(thf)_2]$ (**2b**) in $CDCl_3$ at T = 300 K.

1.6 $[BeI_2(thf)_2]$ (2c):

1.6.1 Solvent – thf-*d8*

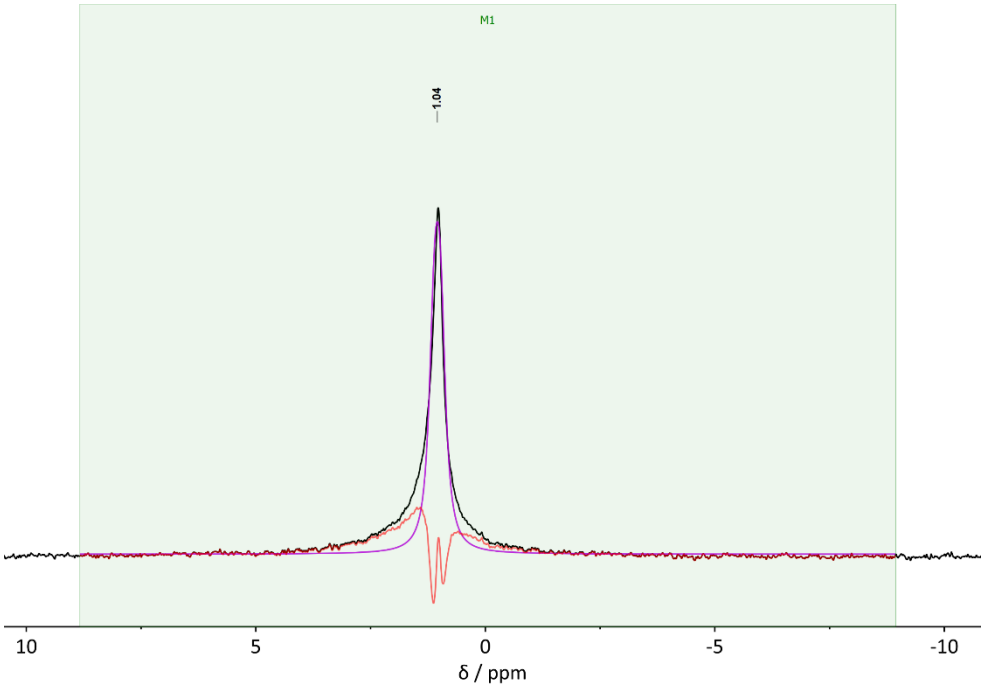

Figure 54: ^{9}Be NMR spectrum of $[BeI_2(thf)_2]$ (**2c**) in thf-*d8* at T = 300 K. Line fitting profiles (purple) and differential plot of calculated *versus* observed line (red) profiles are marked.

1.6.2 Solvent – C_6D_6

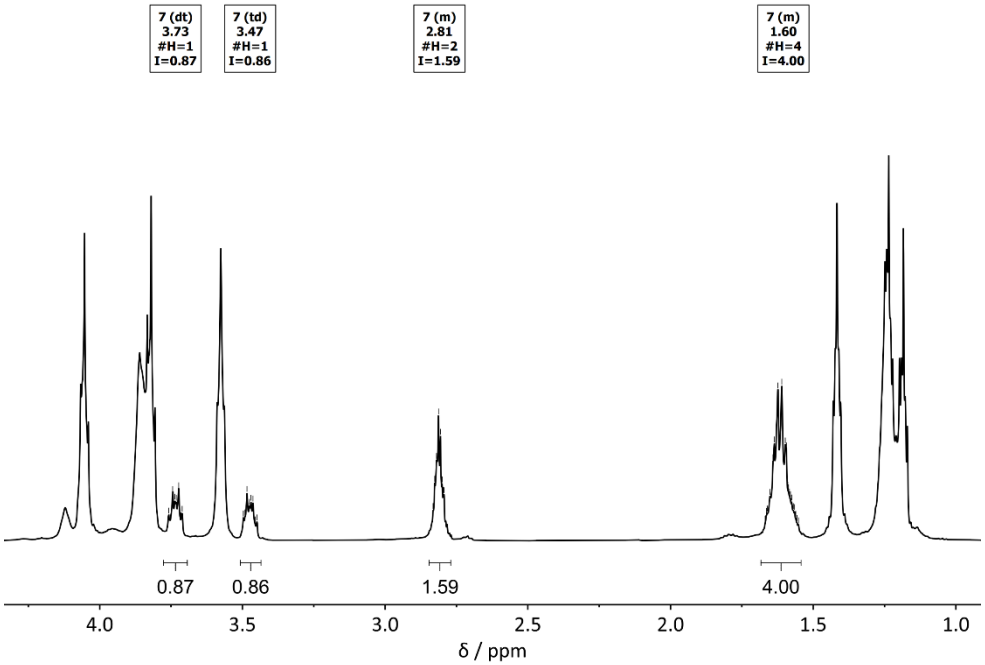

Figure 55: ^{1}H NMR spectrum of Mixture of $[BeI_2(thf)_2]$ (**2c**), $[BeI(thf)_3]^+$ (**4**), $[Be(thf)_4]^{2+}$ (**5**), and $[Be(\mu_2\text{-}O(CH_2)_4I)I(thf)]_2$ (**6**) in C_6D_6 at T = 300 K. Signals corresponding to **7** are marked with the integer 7. Markers for **2c**, **4**, **5** and **6** are omitted for clarity.

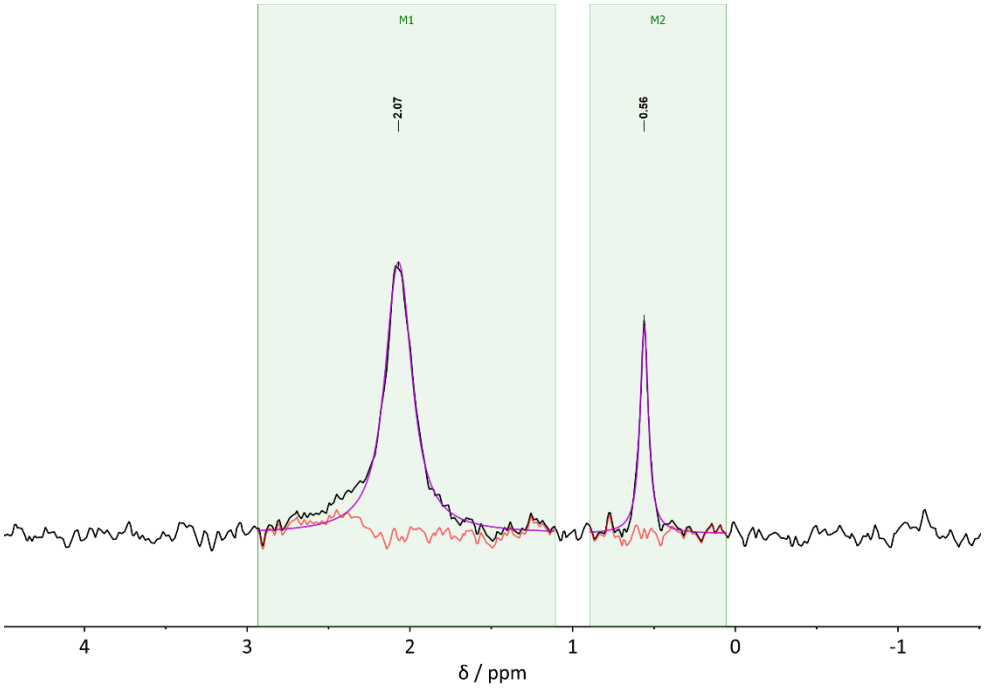

Figure 56: ^{9}Be NMR spectrum of Mixture of $[BeI_2(thf)_2]$ (**2c**), $[BeI(thf)_3]^+$ (**4**), $[Be(thf)_4]^{2+}$ (**5**), and $[Be(\mu_2\text{-}O(CH_2)_4I)I(thf)]_2$ (**6**) in C_6D_6 at T = 300 K. Line fitting profiles (purple) and differential plot of calculated *versus* observed line (red) profiles are marked.

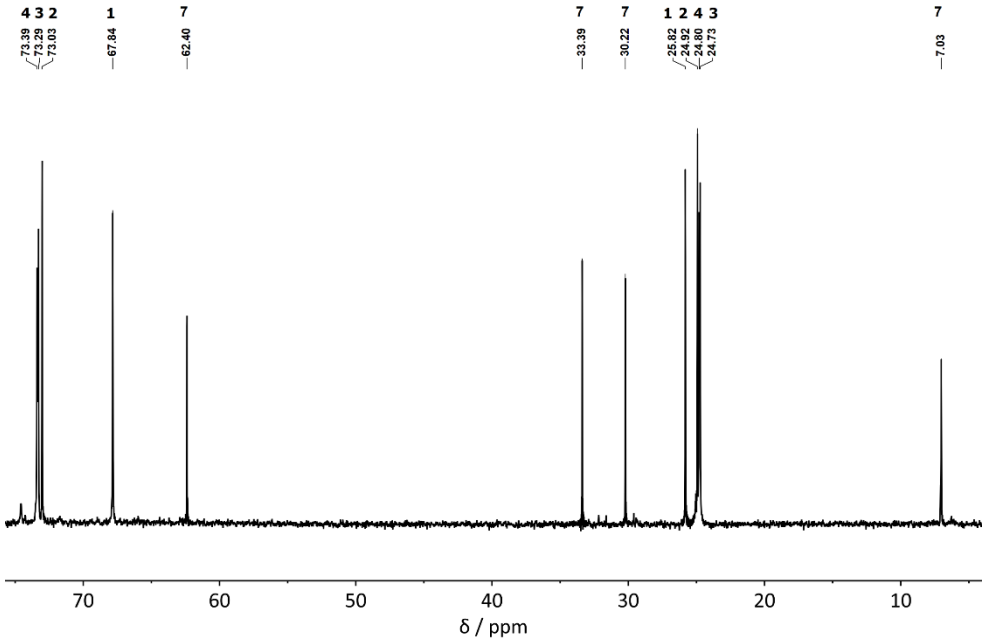

Figure 57: $^{13}C\{^{1}H\}$ NMR spectrum of Mixture of $[BeI_2(thf)_2]$ (**2c**), $[BeI(thf)_3]^+$ (**4**), $[Be(thf)_4]^{2+}$ (**5**), and $[Be(\mu_2\text{-}O(CH_2)_4I)I(thf)]_2$ (**6**) in C_6D_6 at T = 300 K. An assignment of **2c**, **4** and **5** is not possible, but a discrimination of signals of different species is therefore, these sets of signals are marked with the integers 1 to 4. Signals corresponding to **6** are marked with the integer 7.

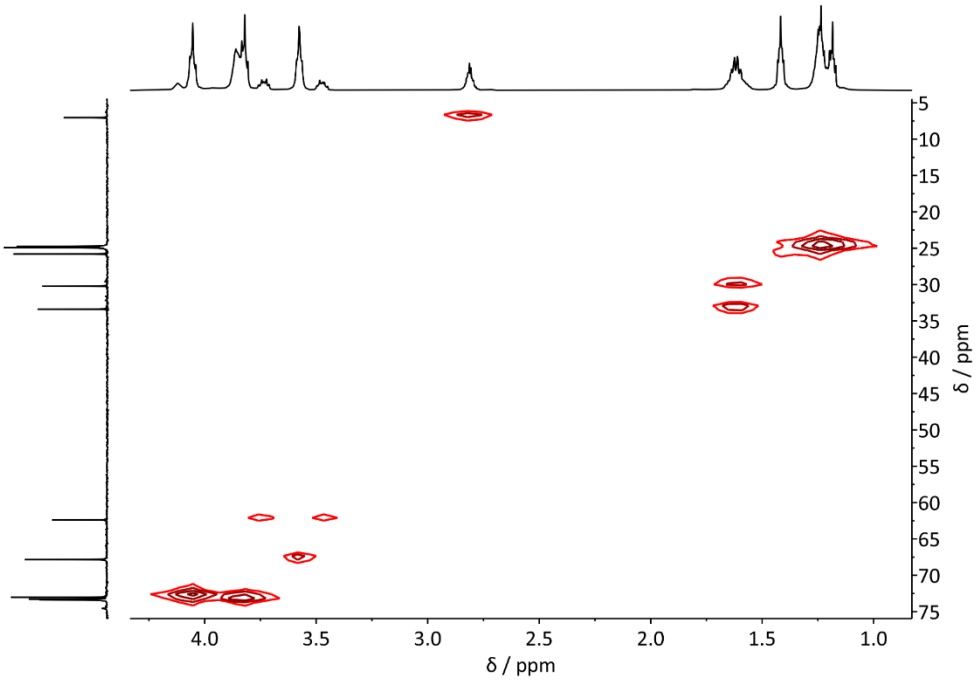

Figure 58: $^{1}H–^{13}C$ HMQC NMR spectrum of $[BeI_2(thf)_2]$ (**2c**) in C_6D_6 at T = 300 K.

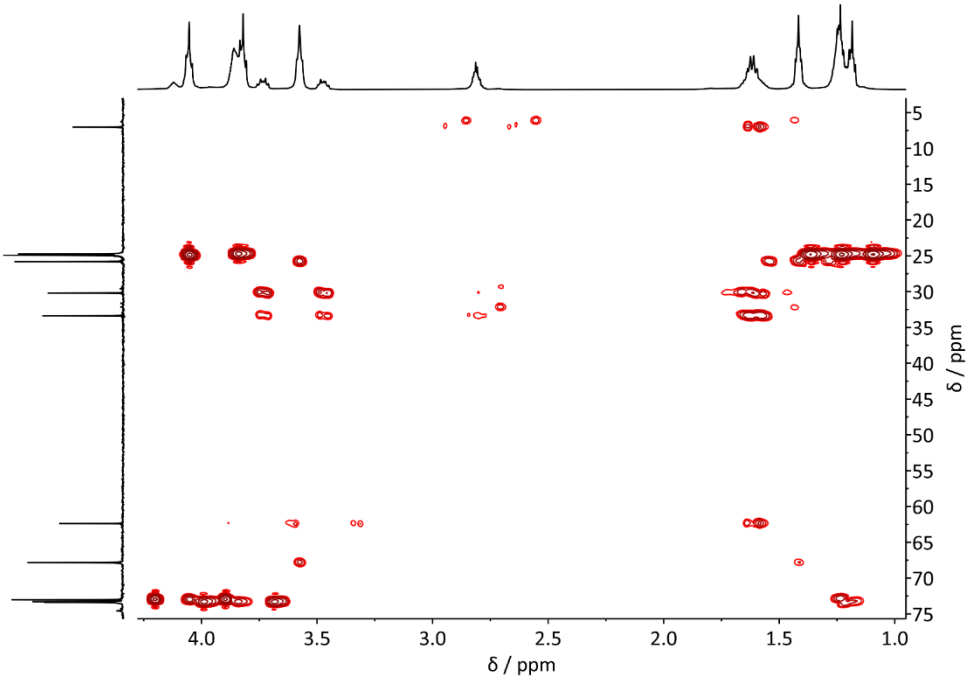

Figure 59: $^{1}H-^{13}C$ HMBC NMR spectrum of $[BeI_2(thf)_2]$ (**2c**) in C_6D_6 at T = 300 K.

1.6.3 Solvent – $CDCl_3$

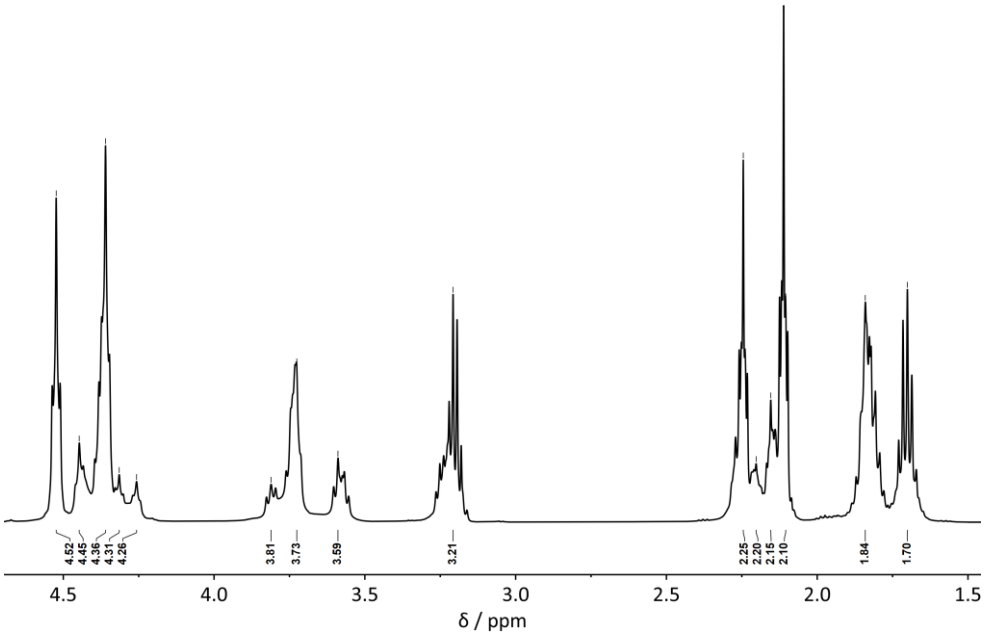

Figure 60: ^{1}H NMR spectrum of $[BeI_2(thf)_2]$ (**2c**) in $CDCl_3$ at T = 300 K. Centers of multiplets are marked with the respective chemical shift below the resonance for clarity.

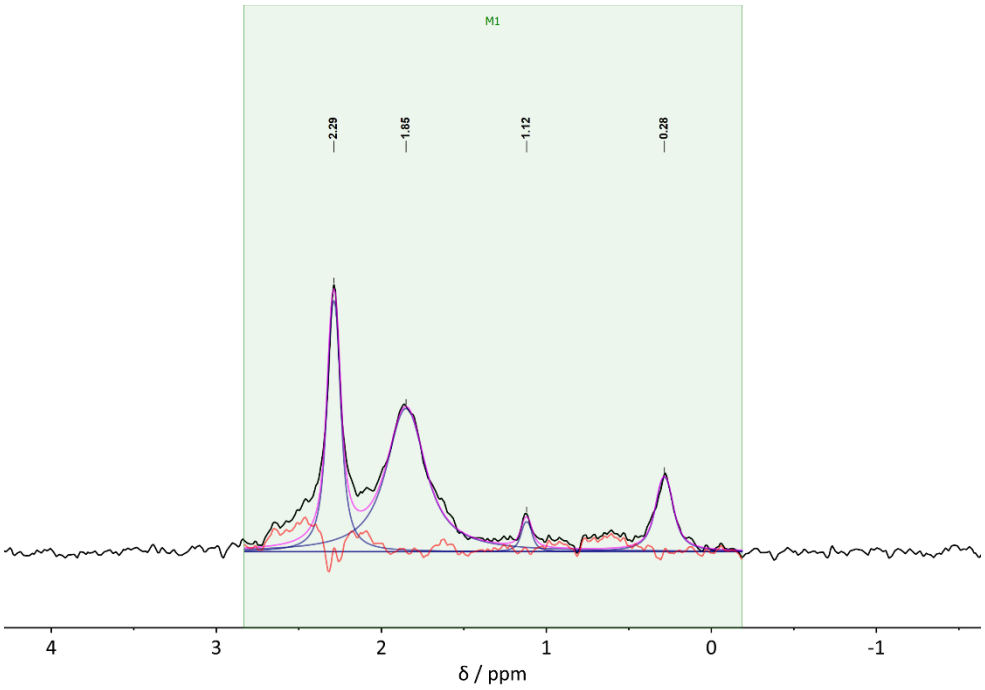

Figure 61: ^{9}Be NMR spectrum of [$BeI_2(thf)_2$] (**2c**) in $CDCl_3$ at T = 300 K. Summed line fitting profiles (purple), single line fitting profiles (blue) and differential plot of calculated *versus* observed line (red) profiles are marked.

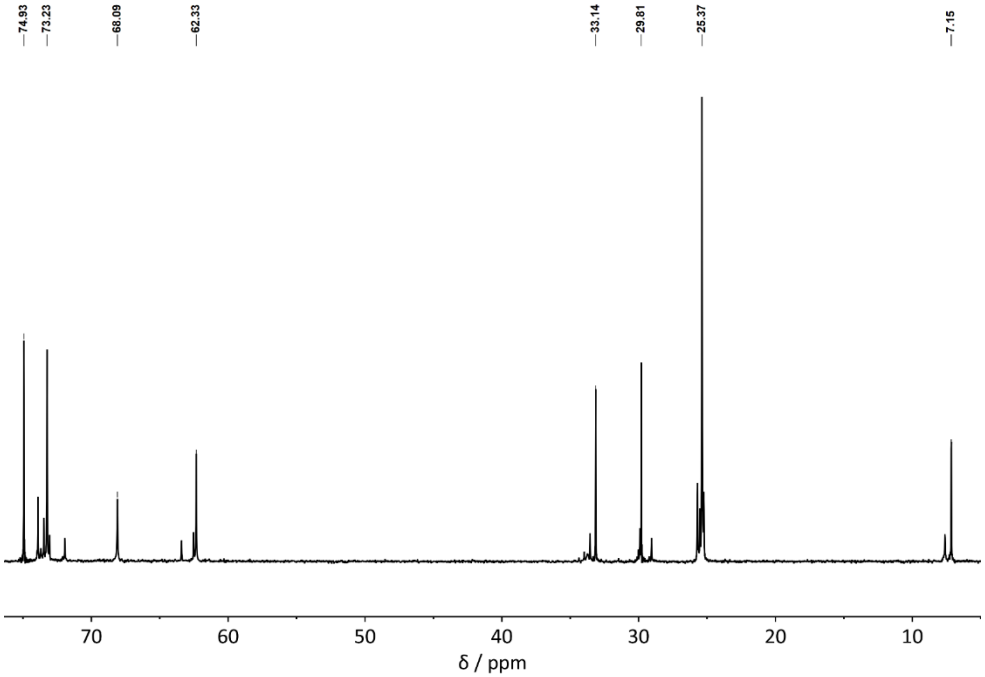

Figure 62: $^{13}C\{^{1}H\}$ NMR spectrum of [$BeI_2(thf)_2$] (**2c**) in $CDCl_3$ at T = 300 K. Only major signals are marked for clarity.

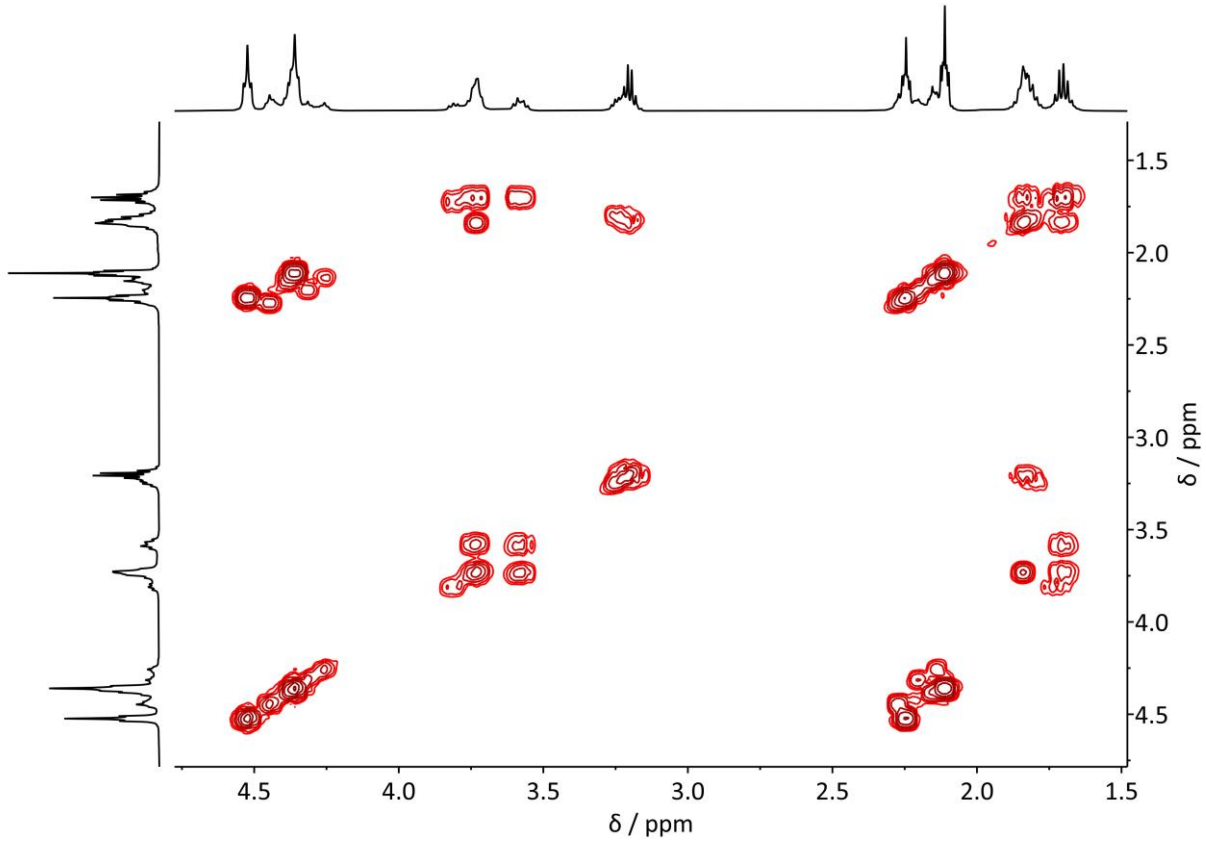

Figure 63: $^{1}H-^{1}H$ COSY NMR spectrum of $[BeI_2(thf)_2]$ (**2c**) in $CDCl_3$ at T = 300 K.

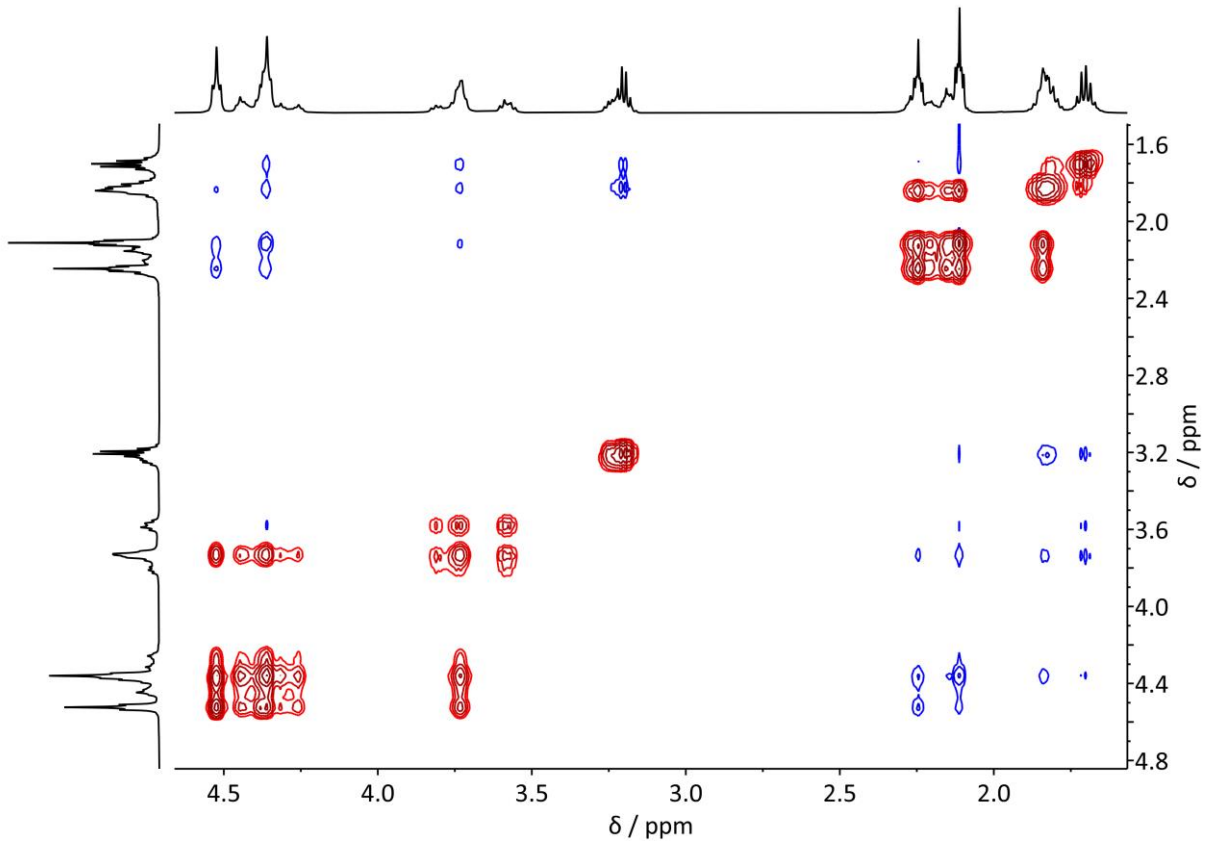

Figure 64: $^{1}H-^{1}H$ EXSY NMR spectrum of $[BeI_2(thf)_2]$ (**2c**) in $CDCl_3$ at T = 300 K. Red signals are positive and blue signals are negative phase.

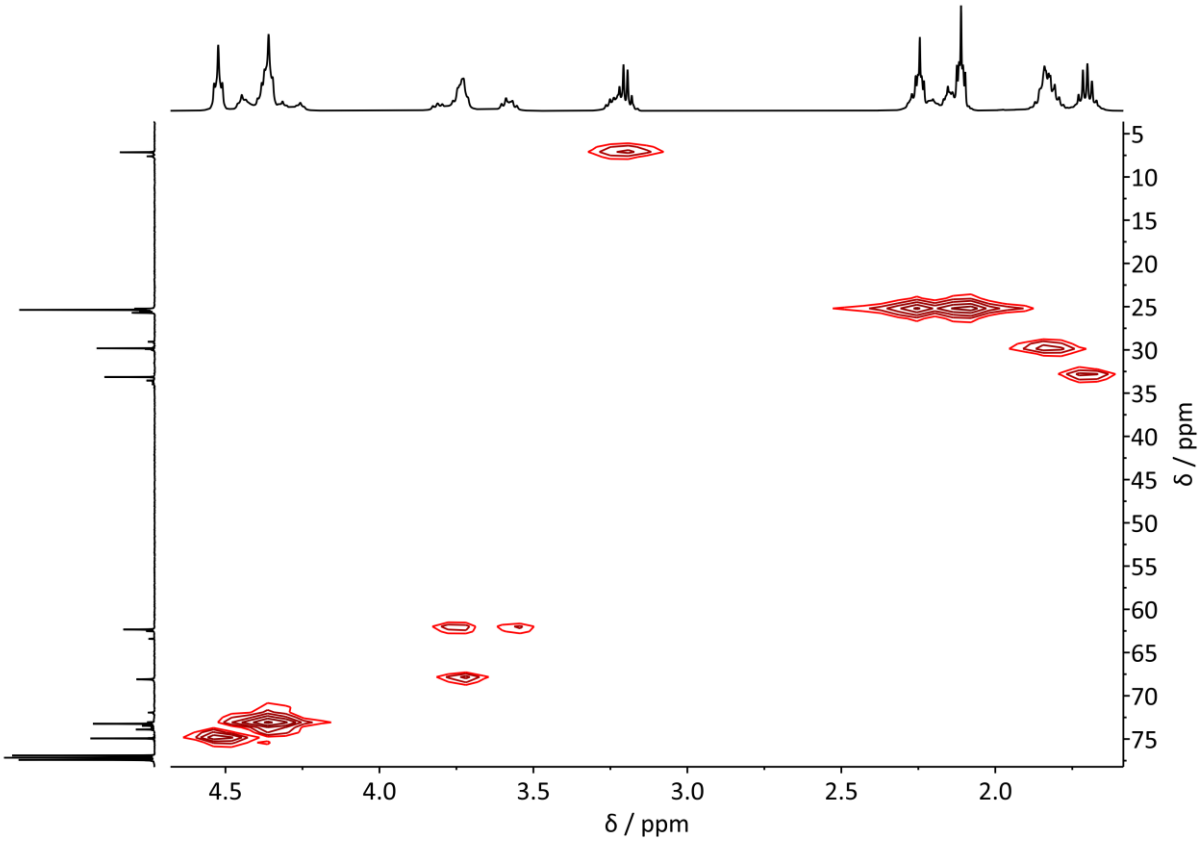

Figure 65: $^{1}H–^{13}C$ HMQC NMR spectrum of $[BeI_2(thf)_2]$ (**2c**) in $CDCl_3$ at T = 300 K.

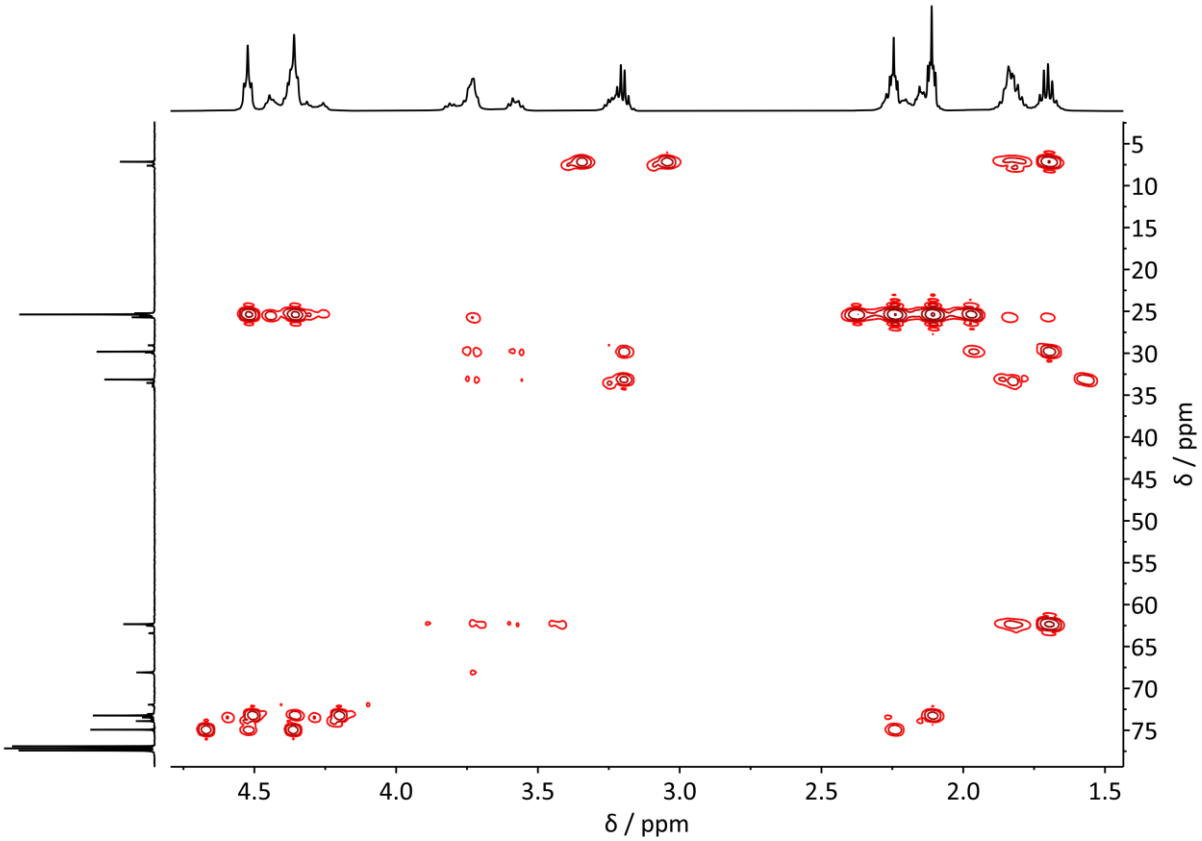

Figure 66: $^{1}H–^{13}C$ HMBC NMR spectrum of $[BeI_2(thf)_2]$ (**2c**) in $CDCl_3$ at T = 300 K.

1.7 $[BeCl_2(OEt_2)]_2$ (3a):

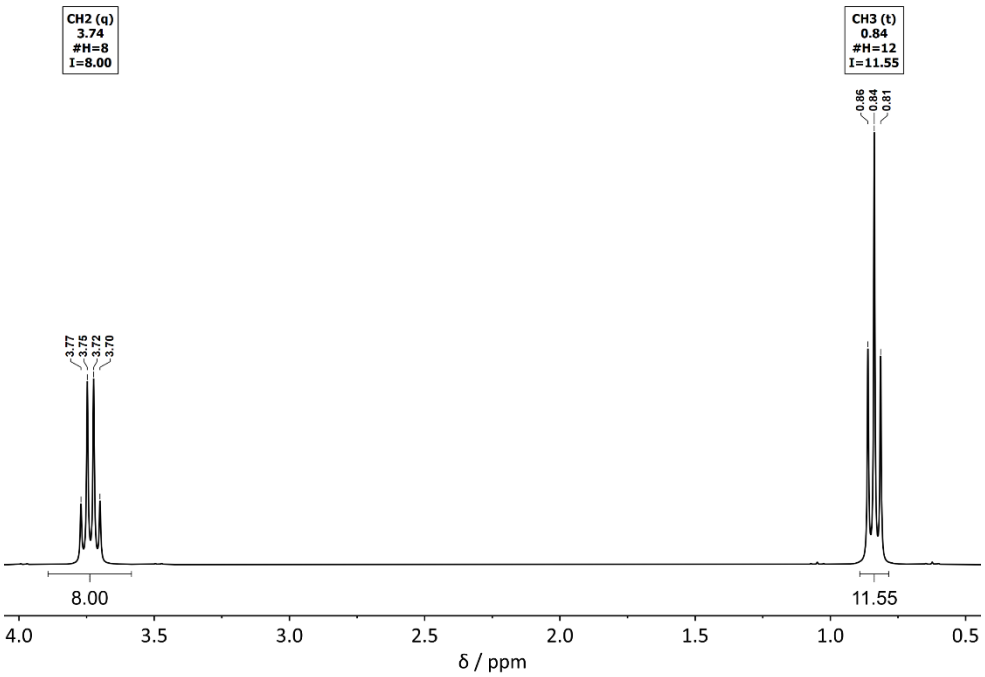

Figure 67: ^{1}H NMR spectrum of $[BeCl_2(OEt_2)]_2$ (**3a**) in C_6D_6 at T = 300 K.

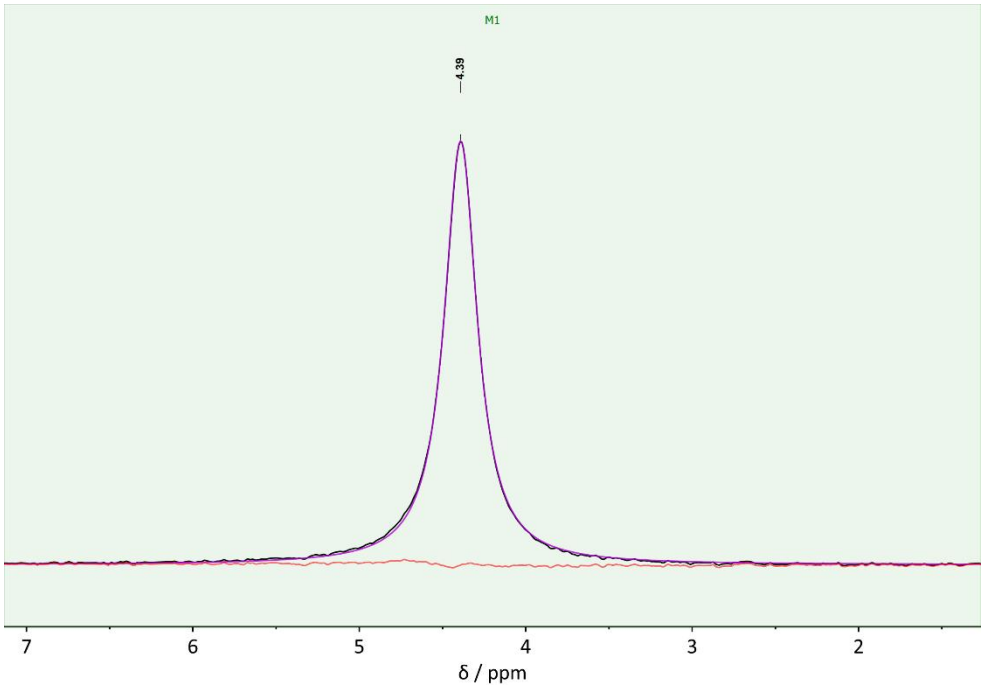

Figure 68: ^{9}Be NMR spectrum of $[BeCl_2(OEt_2)]_2$ (**3a**) in C_6D_6 at T = 300 K.

1.8 $[BeBr_2(OEt_2)]_2$ (3b):

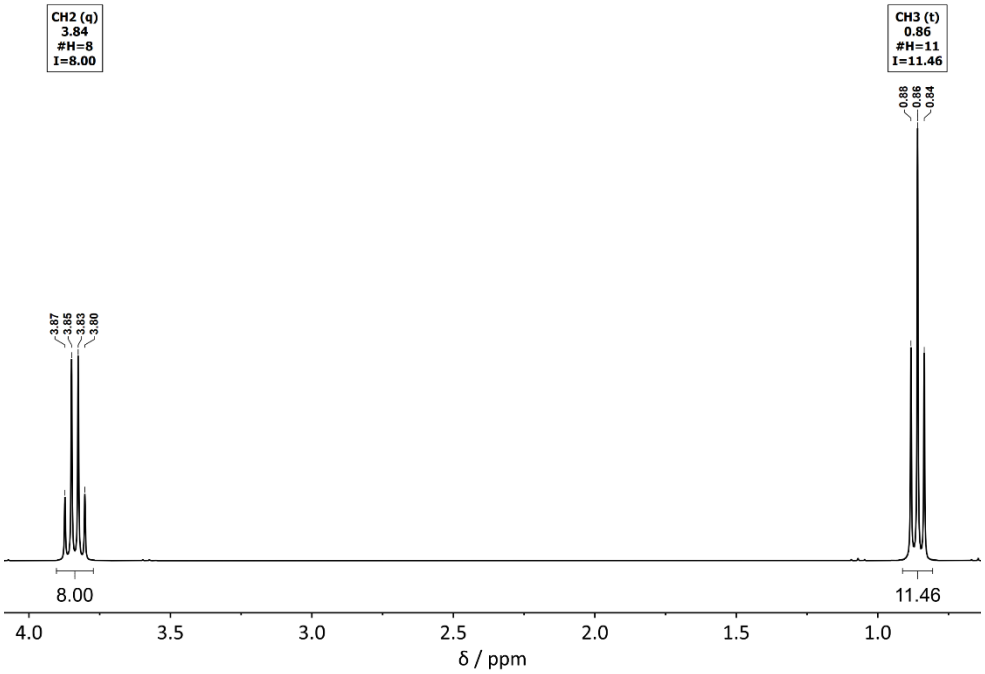

Figure 69: ^{1}H NMR spectrum of $[BeBr_2(OEt_2)]_2$ (**3b**) in C_6D_6 at T = 300 K.

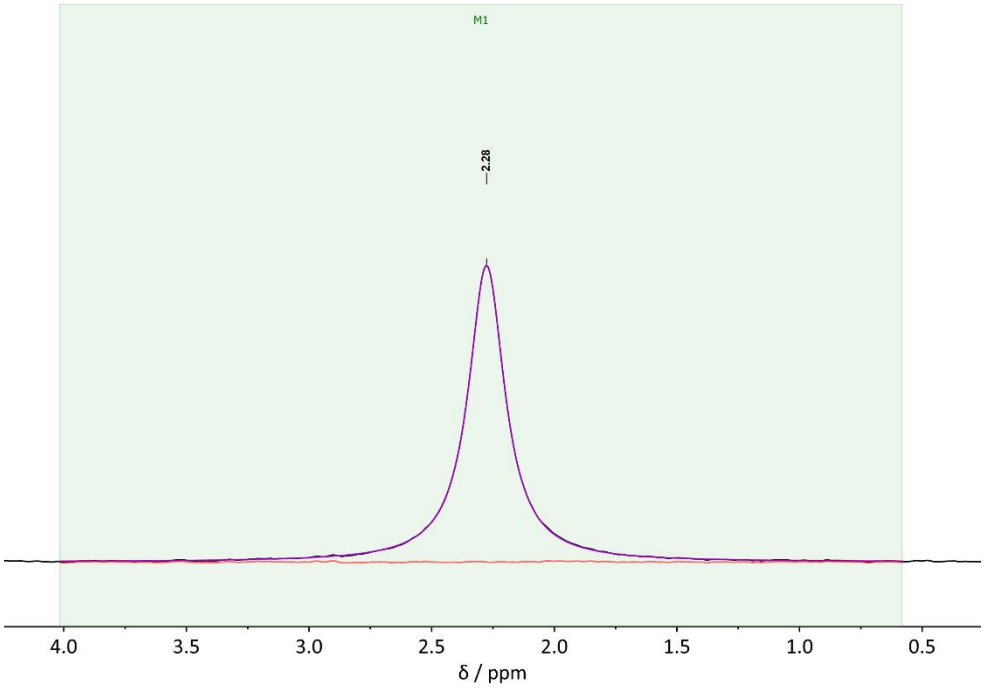

Figure 70: ^{9}Be NMR spectrum of $[BeBr_2(OEt_2)]_2$ (**3b**) in C_6D_6 at T = 300 K.

1.9 $[BeI_2(OEt_2)]_2$ (3c):

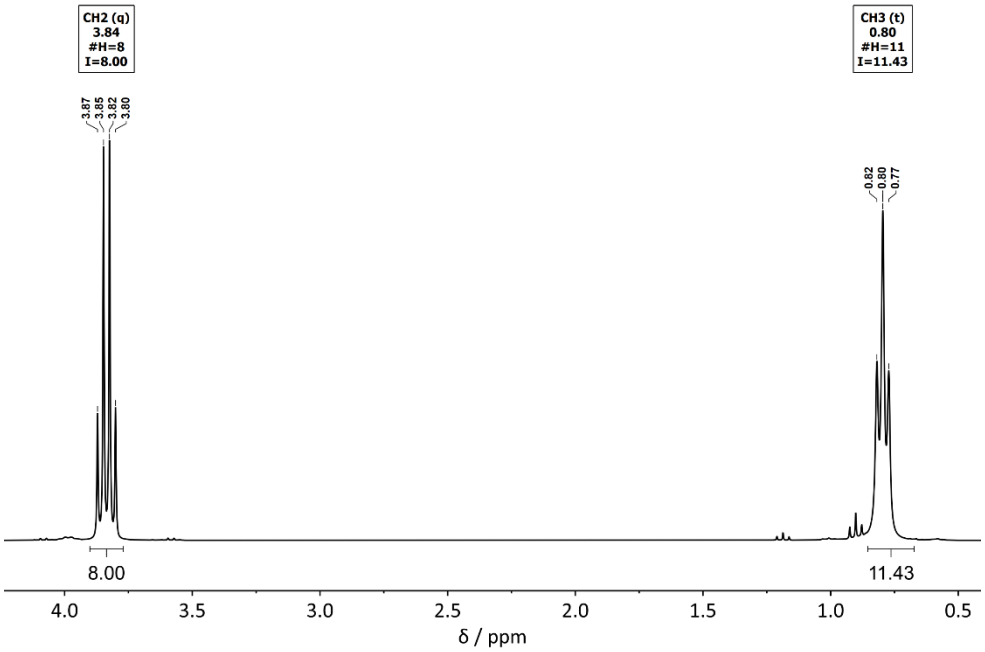

Figure 71: ^{1}H NMR spectrum of $[BeI_2(OEt_2)]_2$ (**3c**) in C_6D_6 at T = 300 K.

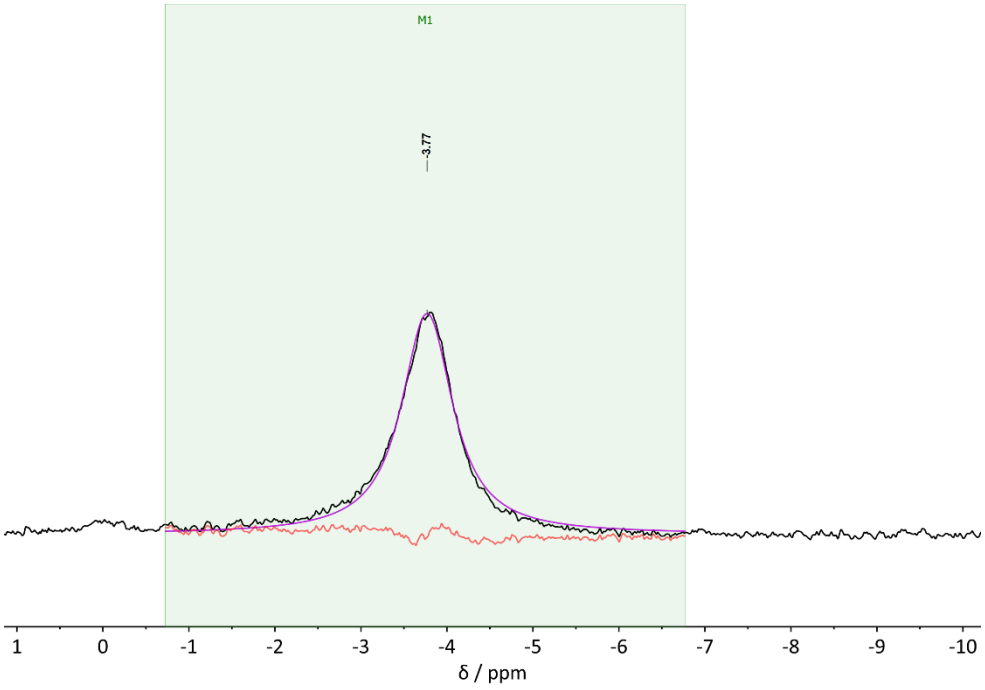

Figure 72: ^{9}Be NMR spectrum of $[BeI_2(OEt_2)]_2$ (**3c**) in C_6D_6 at T = 300 K.

2 Vibrational Spectroscopic Data

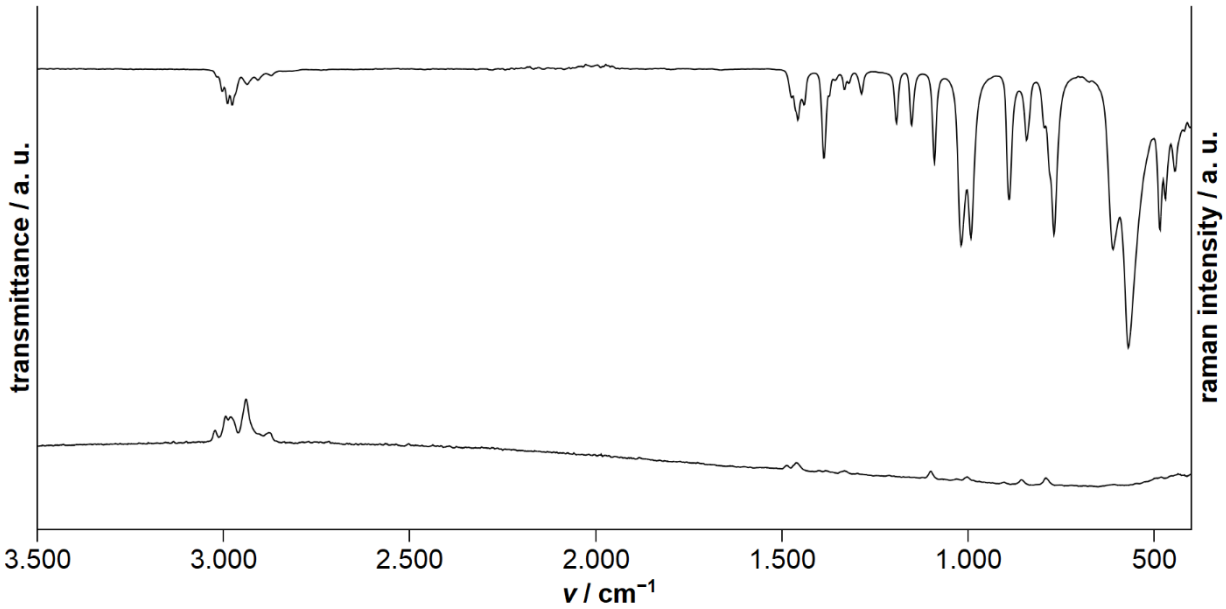

Figure 73: IR (top) and Raman (bottom) spectrum of $[BeBr_2(OEt_2)_2]$ (**1b**).

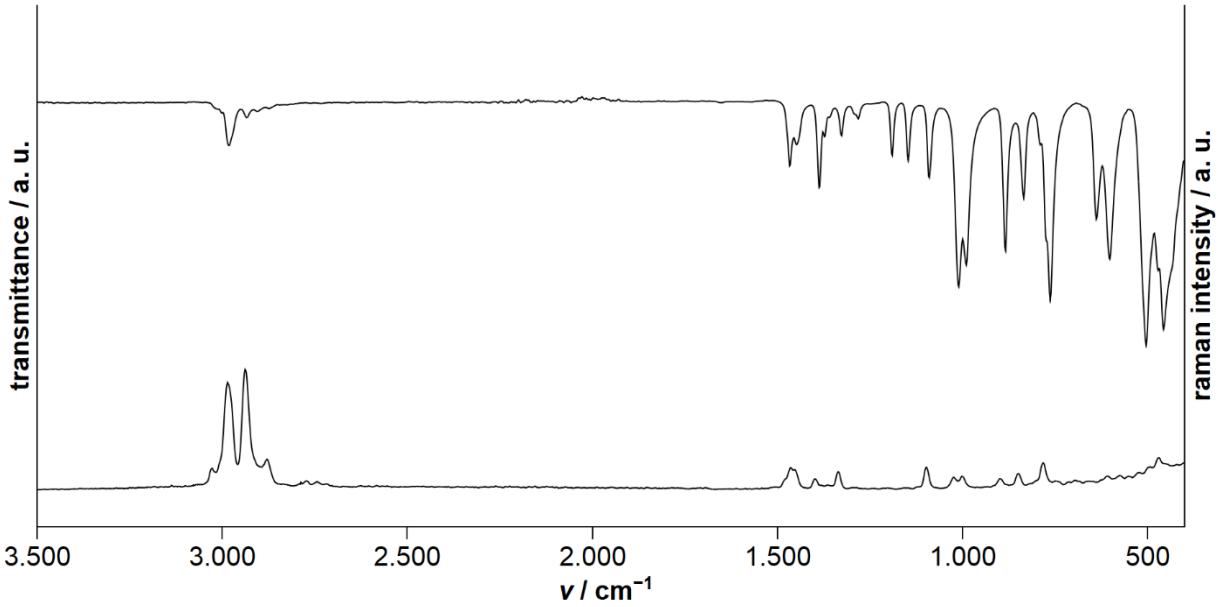

Figure 74: IR (top) and Raman (bottom) spectrum of $[BeI_2(OEt_2)_2]$ (**1c**).

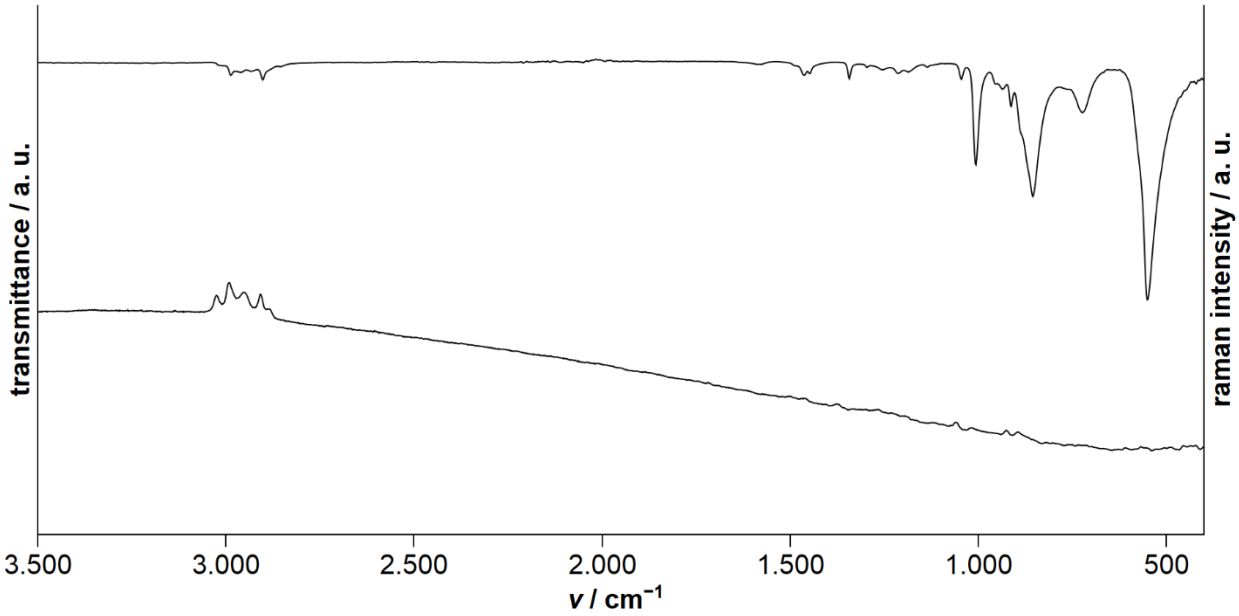

Figure 75: IR (top) and Raman (bottom) spectrum of $[BeBr_2(thf)_2]$ (**2b**).

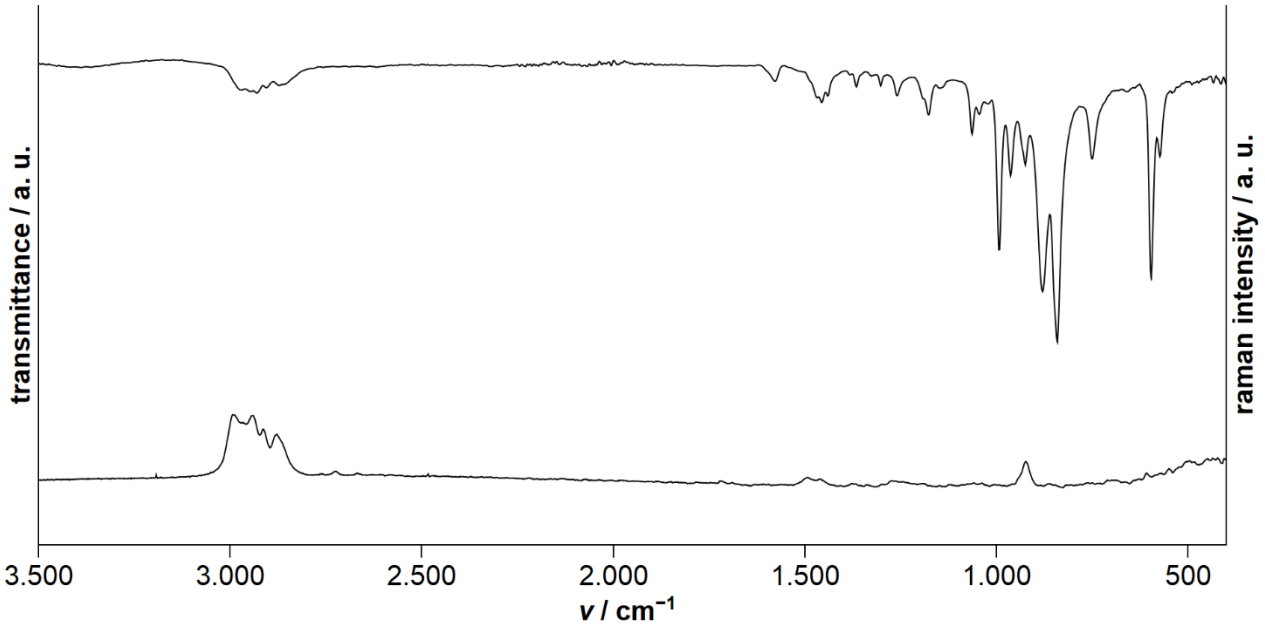

Figure 76: IR (top) and Raman (bottom) spectrum of $[BeI_2(thf)_2]$ (**2c**).